To the Graduate Council:

I am submitting herewith a thesis written by Jason Harold Foster entitled “Model Reduction Techniques for Fluid Dynamical Flow Based PDE Control Problems.” I have examined the final electronic copy of this thesis for form and content and recommend that it be accepted in partial fulfillment of the requirements for the degree of Master of Science, with a major in Electrical Engineering.

_____
Seddik M. Djouadi, Major Professor

We have read this thesis
And recommend its acceptance:

J. Douglas Birdwell

Vasilios Alexiades

Accepted for the Council:

Carolyn R. Hodges

Vice Provost and Dean of the Graduate School

(Original signatures are on file with official student records.)

Model Reduction Techniques for Fluid Dynamical Flow Based PDE Control Problems

A Thesis Presented for
the Master of Science
Degree
The University of Tennessee, Knoxville

Jason Harold Foster
August 2007

Copyright © 2007 by Jason Foster

ACKNOWLEDGEMENTS

I would like to thank the researchers Dr. Chris Camphouse and Dr. James Myatt at the Air Force Research Laboratory for providing the full order system model. Additional thanks goes to my advisor Dr. Seddik Djouadi for giving me the idea to pursue this research and continued help and direction in the areas of model reduction and robust control. I would like to thank my other committee members Dr. Doug Birdwell and Dr. Vasilios Alexiades for their very helpful comments. Further, I would like to thank Dr. Douglas Lawrence for giving the background work on using the ERA method and empirical balancing to solve the one-dimensional Burger's equation. This was invaluable in applying the method to the two-dimensional Burger's equation.

In all things I give thanks to the Living God. Without His care and protection, I would not be able to live a single day. I want to also thank my loving wife who has shown great understanding and patience with this work. Jessica has been my best friend and constant source of strength through this entire process. The completion of this work is a testimony to her continued support every day. Last but certainly not least, I thank my parents for always encouraging me and giving me the tools that I needed to succeed in all of my endeavors.

ABSTRACT

This thesis deals with the practical and theoretical implications of model reduction for aerodynamical flow based control problems. Various aspects of model reduction are discussed that apply to Partial Differential Equation (PDE) based models in general. Specifically, the Proper Orthogonal Decomposition (POD) of a high dimension system is discussed as well as frequency domain identification methods are discussed for initial model creation. Projections on the POD basis give a Galerkin model. Then, the methods of balanced truncation and Hankel optimal norm reduction are applied to the Galerkin model. A state space model is formed by a Galerkin projection of the governing equations and initial conditions onto the POD basis. Further, the weak Galerkin model is simulated with white noise to produce inputs to the Eigensystem Realization Algorithm (ERA). This method estimates a system that accurately reproduces the output of the POD based model. Then, balanced truncation is used to show that model reduction is still effective on ERA produced approximated systems. Finally a method of finding empirical controllability and observability Gramians for the approximated system is introduced. After the empirical Gramians are approximately balanced, the necessary transformation matrix can be applied back to the original system. This empirically balanced realization can then be truncated to further reduce the system model size while retaining the most important system dynamics. The effectiveness of the empirically balanced realization for the linearized model is compared with the balanced truncation of the linearized Galerkin model. Finally, conclusions about the relative effectiveness of the model reduction techniques are made and some possible future research directions are discussed.

TABLE OF CONTENTS

Chapter Page

CHAPTER I 1
INTRODUCTION AND PREVIOUS WORK 1
Necessity for Solutions 1
Problem Statement 3
Galerkin Projection 10
Outline of the Thesis 16
CHAPTER II 19
BACKGROUND ON MODEL CREATION AND FLUID DYNAMICS 19
Real World Systems 19
System Identification Preliminaries 19
Measurements 20
Model Interpretation 21
Fluid Dynamics Background 24
Turbulence 24
Navier-Stokes Equations 25
Burger's Equation 26
Computational Fluid Dynamics 27
CHAPTER III 29
MODEL REDUCTION 29
Model Reduction Approaches 29
Simplicity and Accuracy 31
CHAPTER IV 33
MODEL REDUCTION USING BALANCED TRUNCATION AND HANKEL NORM APPROXIMATION 33
Balanced Truncation 33
Hankel Optimal Norm Model Reduction 40
CHAPTER V 45
FREQUENCY DOMAIN REALIZATION TECHNIQUES 45
Empirical Realization Methods 45
Balanced Truncation 55
CHAPTER VI 61
RESULTS AND OBSERVATIONS 61
POD Basis Truncations 61
ERA Method Applied to the Linearized Temporal Model 68
Empirical Balanced Truncation 70
CHAPTER VII 76
CONTROL DESIGN FOR PDE's 76
LQR Control Formulation 76
LQR Control Results 78
CHAPTER VIII 82
CONCLUSION 82

Methodology 82
Choosing Modes 83
Model Reduction Technique's Relative Effectiveness 84
Future Research Opportunities 85
LIST OF REFERENCES 87
VITA 93

LIST OF TABLES

Table Page

Table 1. Balanced Truncation and Hankel Model Reduction Error Bounds…67
Table 2. System Identification ERA Parameters Used……...70
Table 3. Emperical Gramain ERA Parameters Used……..73

LIST OF FIGURES

Figure Page

Figure 1. Diagram of the Problem Geometry……..…4
Figure 2. Boundary Inputs for System Identification for Snapshot Creation……..7
Figure 3. First 100 Singular Values of the Correlation Matrix, L……10
Figure 4. First 25 POD Modes……11
Figure 5. Comparison of 40-Order Galerkin Model and Full Order Snapshot Model Flow Solutions……..……15
Figure 6. Nonlinear and Linearized Galerkin 40th Order Flow Solutions……..17
Figure 7. System with Insufficient Measurements for System Identification……23
Figure 8. Model Reduction Paths……30
Figure 9. State Space Realization Separating Inputs……..35
Figure 10. Excitation Inputs for ERA Method ……...54
Figure 11. ERA Method Steps Block Diagram ……54
Figure 12. The Empirical Balanced Truncation Method ……58
Figure 13. Comparison of Full Order HSVs and Hankel Optimal Norm HSVs…62
Figure 14. Balanced Truncated and Hankel Approximation Difference ……..63
Figure 15. Output Comparison of Reduced Models to Nonlinear 40 Order Model……..64
Figure 16. Temporal Model Flow Comparisons……...67
Figure 17. ERA Estimated System Balanced Truncation.....69
Figure 18. ERA Estimated System Output Approximation From Galerkin Model ……..69
Figure 19. Linearized Galerkin and Empirically Balanced System's HSVs ……72
Figure 20. First 5 Outputs for Temporal and Empirically Balanced Truncated...72
Figure 21. Validation of Empirical Balanced Truncation……74
Figure 22. Flow Comparison: Standard Versus Empirical Balanced Truncation……..75
Figure 23. Desired Reference Flow for Control and Initial Flow Condition 78
Figure 24. Control Applied to the Balanced Truncation Reduced Model……80
Figure 25. Control Applied to the Hankel Optimal Norm Approximation Reduced Model ……81

CHAPTER I
INTRODUCTION AND PREVIOUS WORK

Necessity for Solutions

Significant attention has recently been given to the topic of reduced order modeling since it can be used in various applications. Further, additions to literature in this area seem to be continuing ([19], [15], [3], [12], [16]). One such application of reduced order modeling is control design in the context of aerodynamic flow. Aerodynamic flow control is a research area of great interest to the fluid mechanics community. Presently considerable research efforts are working with feedback control law design for systems described by PDEs that need a very large number of states to accurately simulate their characteristics. Recent advances in the design of actuators and sensors can be leveraged for better system control only if the control design methods provide a reliable low order controller [4]. Additionally, simulation, and experimental diagnostics are making applications such as the suppression of acoustic tones in cavities, and trajectory control without the need to move hinged surfaces a possibility [5].

The traditional systematic development of feedback control law for these systems subject to a large number of states is currently an intractable problem. Reduced models are important for the design of feedback control laws, which rely on models that capture the relevant dynamics of the input-output system and are amenable to control design. In addition, many applications require the integration of feedback control to achieve robustness to flight condition and vehicle attitude, precision tracking, overcoming low-fidelity models, or moving a system away from a stable solution or limit cycle as efficiently as possible [5].

Feedback control strategies offer the possibility to improve performance and reduce control power through the control of unstable structures in the flow field.

Unfortunately, it is very difficult to create models that capture the relevant dynamics of the input-output system. For example, computational fluid dynamics simulations can provide good solutions to a discretized version of the Navier-Stokes equation [33], [35]. However, accurate simulations for simple shapes such as two-dimensional airfoils, or complex shapes, such as a full vehicle, require several thousands to millions of states. Therefore, the simulation results are not directly useful for control design [5]. Complexity in the model is a legitimate need. The large number of states is necessary to capture important flow features that occur at extremely small spatial scales. Although these small flow features might seem insignificant, if they are not captured, it is not possible to analyze if they are necessary in securing the closed loop system's overall stability [4].

Another challenge for designing control laws for flow control is that the Navier-Stokes equations in traditional form are not affine. Therefore, it is necessary to separate the portions of the discretized system where the control input enters the system for control design. Systematic control design for boundary controls is currently an open problem. Often the controls are simply specified by open loop forcing [24]. Unfortunately, some physical devices such as actuators and airfoils are physically limited to the boundary [5]. Boundary feedback control is described in [4] where boundary feedback control laws were developed using a linear quadratic regulator (LQR) control formulation with the weak formulation of Proper Orthogonal Decomposition (POD) system models.

POD has been extensively investigated in distributed parameters systems due to its order reduction capability [28]-[32], and balanced truncation, which is a simple yet efficient model reduction technique widely used in reducing model orders of high order linear systems [20], [22], [23]. POD models of only a few dozen states can often accurately capture the input-output behavior of systems that have full order system models of thousands of states [5].

In addition to using the POD method in conjunction with model reduction techniques, the idea of using empirical Gramians is growing in popularity for use in an approximate balanced truncation [14], [15], [27], [36]. Further some work has been done on finding nonlinear empirical Gramians for balanced truncation [36], [37].

In the fluid mechanics community, balanced truncation has been applied, for example, to unsteady motion of a two-dimensional airfoil [33]. Also, a version of a balanced POD has been applied to modeling turbulent and laminar plane channel flows [12]. This method is referred to as a traveling POD. In this case the standard POD function is modified to shift to dynamically aligning itself with a predetermined function based upon the previous POD mode calculated.

Unfortunately, it might not be possible or practical to actuate over an entire problem region. In the area of fluid mechanics controls must often be fixed to the boundary of the problem geometry. The problem geometry used for this thesis is one example of a case where control is restricted to the boundaries by physical necessity.

Problem Statement

The problem statement for aerodynamic flow control can often have an obstacle that physically imposes a condition that only allows boundary control. The specific problem geometry considered in this thesis is shown in figure 1. The idea and methods presented here could be modified to apply to a different geometry or obstacle shape. The problem statement with its corresponding boundary conditions and governing equations was taken from [4]. A realistic example of this geometry in an aerodynamic application would be a payload hatch open during flight with actuator control only on the boundary. Let Ω_{gap} be the region defined by $[a_1, a_2] \times [b_1, b_2]$. Let Ω_{full} be the region defined by $(a_0, a_{end}) \times (b_0, b_{end})$.

Then the problem domain is given by $\Omega = \Omega_{full} / \Omega_{gap}$. In this problem setup, Ω_{gap} is an obstacle.

The system dynamics that act within the problem domain are described by the two dimensional Burger's equation [4]:

$$\frac{\partial}{\partial t} w(t,x,y) + \nabla \bullet F(w) = \frac{1}{r}\left(\frac{\partial^2}{\partial x^2} w(t,x,y) + \frac{\partial^2}{\partial y^2} w(t,x,y) \right), \tag{1.1}$$

where the form of F(w) is

$$F(w) = \left[c_1 \frac{w^2(t,x,y)}{2} \qquad c_2 \frac{w^2(t,x,y)}{2} \right]^T, \tag{1.2}$$

In this case, the value for c_1 is equal to 1 and c_2 is equal to 0. The value r is similar to the Reynolds number used in the Navier-Stokes Equation. This parameter controls how much nonlinearity is present in the problem. The value used in this thesis is 300, a small "Reynolds number" but it still allows for the nonlinearity to show in the problem.

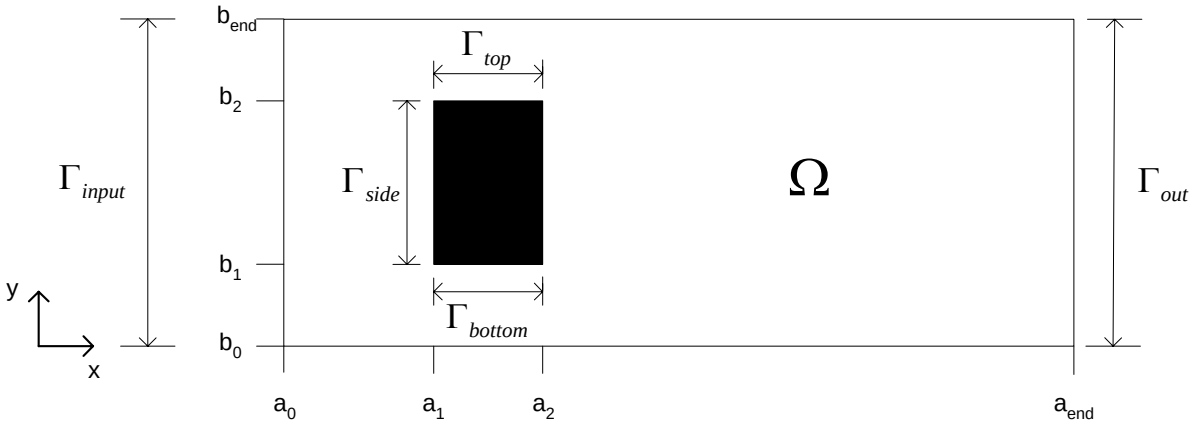


Figure 1. Diagram of the Problem Geometry

Dirichlet boundary conditions located on the obstacle top and bottom are denoted by Γ_{top} and Γ_{bottom}. A Dirichlet boundary condition is a first-type boundary condition that specifies the values of the solution defined by f(x) on a domain boundary [13]. The form of the boundary condition is

$$w(t,x,y) = f(t,x,y) \quad \forall (x,y) \in \partial\Omega \tag{1.3}$$

The boundary conditions on the top and bottom are described by the following equations:

$$w(t,\Gamma_{bottom}) = u_{bottom}(t)\Psi_{bottom}(x), \tag{1.4}$$

$$w(t,\Gamma_{top}) = u_{top}(t)\Psi_{top}(x). \tag{1.5}$$

Here $u_{top}(t)$ and $u_{bottom}(t)$ are the time varying control inputs on the top and bottom boundaries respectively. Further, $\Psi_{top}(x)$ and $\Psi_{bottom}(x)$ describe the spatial effect that the controls have on the top and bottom boundaries.

The boundary condition on the airflow intake side is

$$w(t,\Gamma_{in}) = f(y) \tag{1.6}$$

and it is parabolic in nature. The airflow outtake side has a Neumann boundary condition that has the form [13]

$$\frac{\partial}{\partial x} w(t,\Gamma_{out}) = 0. \tag{1.7}$$

On all of the remaining boundaries of Ω, $w(t,x,y)$ is set equal to 0 for all values of t. Finally, the initial conditions for the interior are given by

$$w(0,x,y) = w_0(x,y) \in L^2(\Omega). \tag{1.8}$$

A numerical solution was found by simulation using a uniformly spaced grid. The resulting system model contains a little more than 2000 states. After this a method of optimal (with respect to average kinetic energy [10]) subspace detection was performed. POD is a method for model reduction that works on the idea that a set of basis vectors in an infinite dimensional space can be created that gives the best representation of typical system behavior for a fixed basis dimension size [10]. The method used for determining how many modes need to

be retained is a design choice. A reasonable choice and the one used in this POD model construction were to look at the total energy captured. When a vector having significant system "energy" was found, it was forced to be perpendicular to all previously found $\varphi_k's$. A condition that 99.9% of system energy must be captured was used for determining how many system modes were needed. This condition was met by a 40 state POD basis. Although this is a major reduction from the numeric solution, it will be shown that the most important system dynamics can be retained with even lower state number system models.

Other names for this decomposition are the Karhunen-Loeve decomposition, [40] [41], and principal component analysis [42]. Some applications have been in fluid mechanics, random variables, image processing, and data compression [10]. This decomposition method has been used extensively ([1], [4], [5], [7], [12], [19], [35]) to analyze experimental or simulation data and to extract the most dominant trends. For the case of turbulent flows these trends are the most important features in space and time. A short description of this methodology follows, but a more complete description is found in chapter IV. The general approach of this method is to construct a series of solution "snapshots." These snapshots are solved by numeric simulations of the governing system equation(s) with a variety of input equations. The method of finding these solution snapshots is described in detail in [19], [38]. The greatest strength of this method is that it provides a relevant and optimal set of basis functions that allows a low-dimensional subspace to be identified. This subspace will allow model creation when the governing equations are projected onto the created subspace [10]. The snapshots are needed for the creation of a correlation matrix that can be used to find the important system information. It is important to choose relevant input signals for the numerically simulated system. Further, these inputs should be similar to the expected inputs of the real system. In this way, the POD model should accurately represent the system in the normal operating range. In this case the inputs used for system identification are of the form [4]

$$u_{bottom}(t) = \beta \sin(0.25t^2) \qquad u_{top}(t) = 0, \tag{1.9}$$

$$u_{bottom}(t) = 0 \qquad u_{top}(t) = \beta \sin(0.25t^2), \tag{1.10}$$

$$u_{bottom}(t) = \beta \sin(0.25t^2) \qquad u_{top}(t) = \beta \sin(0.25t^2)\ , \tag{1.11}$$

where the values for β are –3, -2, and –1 and the range for t is 0 to 10 seconds with a sample every 50 milliseconds. The squelch signal for all three values of β is shown in figure 2.

The numerical simulation was performed to create the ensemble of solution snapshots $\{S_k(x,y)\}_{k=1}^{M}$ [4]. The snapshots refer to a collection of samples at specific points of individual solutions to the governing equation [10].

Each snapshot captures samples at the specific points on the problem geometry while the control inputs are varied. The value for M (the number of snapshots) must be greater than the number of modes that one will choose for the approximated system model. For a good representation, the size of M should be much larger than the ultimately desired size for the POD basis [4].

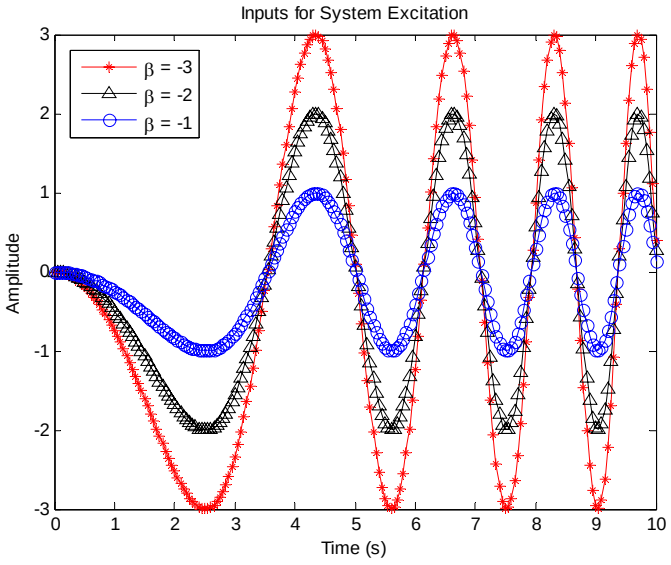


Figure 2. Boundary Inputs for System Identification for Snapshot Creation

This ensemble is constructed as described in ([4] and [10]). The solution to the PDE lies in an infinite dimensional space and can be approximated within the optimal finite dimensional subspace as

$$w(t,x,y) \approx \sum_{k=1}^{N} \alpha_k(t)\varphi_k(x,y) \tag{1.12}$$

where the α_k's are time varying coefficients that multiply the POD basis vectors φ_k's. Therefore, the solution is described as a linear combination of the identified basis vectors. The ultimate goal for finding a solution to the governing equations is then to find the α_k's and φ_k's. The correlation matrix L, of size M x M, is composed of the inner products of the snapshots. Then in $L^2(\Omega)$

$$L_{k,j} = \left\langle S_k, S_j \right\rangle \tag{1.13}$$

$$\left\langle S_k, S_j \right\rangle = \int_\Omega S_k S_j^* dx\, dy \tag{1.14}$$

The term ‘ensemble member’ is used to describe one element of the collection of solution snapshots [4].

The POD basis is optimal in the average kinetic energy sense [10]. The function φ_i is chosen to maximize the average projection of the member u_i onto φ_i. This idea is expressed in the following manner [10]

$$\max_{\varphi \in L^2(\Omega)} \frac{\left|\left\langle u_i, \varphi_i \right\rangle\right|^2}{\left\|\varphi_i\right\|^2}. \tag{1.15}$$

Here $\left\langle \right\rangle$ is an averaging operation and $\left\| \right\|$ is the standard L^2 norm.

Unfortunately, this equation only finds the optimal projection on one of the basis functions. The entire set of functions must be looked at concurrently to find the optimal basis.

A choice must be made on how many modes will be kept in the POD constructed subspace. This number can be chosen to be sufficiently large such that the vast

majority of the system's total energy is captured. Additionally this number of modes to keep could be based upon the hardware abilities of the device doing the computations. The chosen number of modes to keep is denoted as N. A singular value decomposition of the matrix L is performed. The N largest eigenvalues $\{\lambda_1, \lambda_2, ..., \lambda_N\}$ of the matrix L are found and placed in descending order. Then the set of eigenvectors are identified to be $\{v_1, v_2, ...v_N\}$. There is a justification for choosing only part of the eigenvalues of the system. The "scree" plot [43] is analogous to the situation that describes the steep descent of a mountain until the "scree" is reached at the bottom. The steep decent portion of the plot shows the "true" principal components. However, after the sharp break in the plot, the remaining principal components can be considered error terms or "false" principal components [43]. The principal components are examined for a definitive change in the slope of their values in figure 3. The sharp break in the slope appears to occur between the 10th and 15th singular values. Therefore, any additional modes that are retained are simply for added certainty that potentially important principal components are retained.

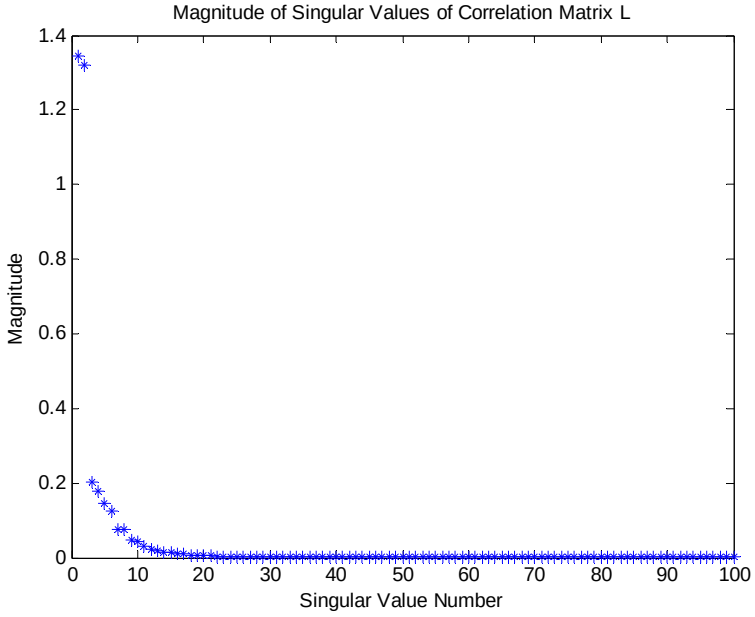


Figure 3. First 100 Singular Values of the Correlation Matrix, L

The resulting orthonormal POD basis of dimension N can be constructed using the information found from the correlation matrix L. First, the eigenvectors of L are weighted by their corresponding eigenvalues and normalized according to [4]

$$\lambda_k \|v_k\|^2 = 1 \text{, for k} = \{1, 2, ..., N\}. \quad (1.16)$$

Then, the POD basis set is formed according to

$$\phi_k(x, y) = \sum_{j=1}^{M} v_{k,j} S_j(x, y), \quad (1.17)$$

with $v_{k,j}$ being the j[th] component of the eigenvector v_k. Solving equation (1.17) gives N φ_k's, which constitute the POD basis of dimension N.

Figure 4 shows the first 25 modes, φ_k's, of the POD basis. The remaining part of the solution to equation (1.12) is the identity of the α_k's. Now that the POD basis for the desired number of dimensions has been found, the original equation must be projected onto this POD basis so that the α_k's can be found.

Galerkin Projection

It is possible to the project the governing equation onto the POD basis. Further, the full order initial condition must be projected onto the POD basis. Therefore, both the equation that is of interest and all of its initial conditions must be projected onto the POD basis. This projection is accomplished with a Galerkin type projection. In some circumstances these Galerkin projections can result in very poor performance. They can even inadvertently cause unstable states and form limit cycles when the original system does not have these problems [19]. The Galerkin projection results in only a weak solution to the PDE. However, this weak solution eventually leads to a state space temporal model using the following procedure as provided in [4].

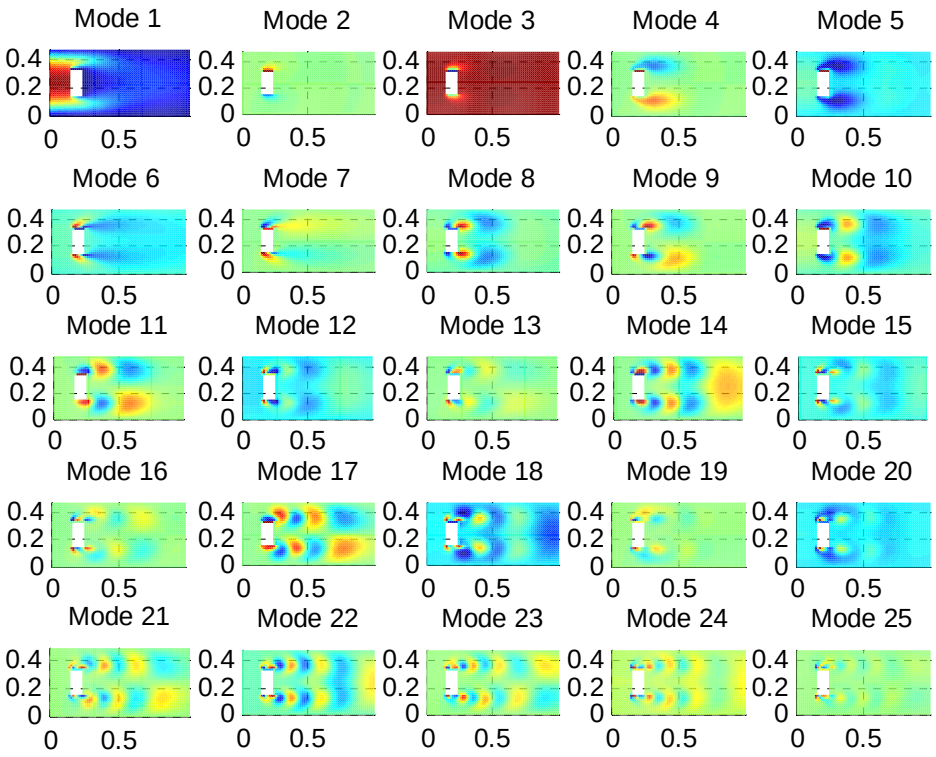


Figure 4. First 25 POD Modes

Equation (1.12) is substituted into equation (1.1), the governing equation for the problem. Then a Galerkin projection is performed which gives a system of ordinary differential equations (ODEs) [4]. Let the solution to the two-dimensional Burgers equation be given by $w(t,x,y)$ as in [4]. Then,

$$\int_{\Omega}\frac{\partial}{\partial t}w(t,x,y)\varphi_k(x,y)dx=\frac{1}{\mathrm{Re}}\left[\int_{\partial\Omega}(\nabla w(t,x,y)\bullet n)\varphi_k(x,y)dA(x)-\int_{\Omega}\nabla w(t,x,y)\bullet\nabla\varphi_k(x,y)dx\right]-$$

$$\left[\int_{\partial\Omega}(F(w)\bullet n)\varphi_k(x,y)dA(x)-\int_{\Omega}F\bullet\nabla\varphi_k(x,y)dx\right], \qquad (1.18)$$

where the first term on the right hand side (rhs) is

$$\int_{\partial\Omega}(\nabla w(t,x,y)\bullet n)\varphi_k(x,y)dA(x)=\int_{a_1}^{a_2}\left(\frac{\partial}{\partial y}w(t,x,b_1)\varphi_k(x,b_1)-\frac{\partial}{\partial y}w(t,x,b_2)\varphi_k(x,b_2)\right)dx$$

$$-\int_{b_0}^{b_{end}}\frac{\partial}{\partial x}w(t,a_0,y)\varphi_k(a_0,y)dy \quad . \qquad (1.19)$$

The Neumann boundary condition forces the portion of the boundary integral over b_0 to b_{end} along a_{end} to be 0. Stated mathematically

$$\int_{b_0}^{b_{end}}\frac{\partial}{\partial x}w(t,a_{end},y)\varphi_k(a_{end},y)dy=0\,. \qquad (1.20)$$

The second boundary integral on the right hand side (rhs) of equation (1.18) is decomposed to the following [4]

$$\int_{\partial\Omega}(F(w)\bullet n)\varphi_k(x,y)dA(x)=\frac{1}{2}\int_{b_0}^{b_{end}}(w(t,a_{end},y)^2\varphi_k(a_{end},y)-f(y)^2\varphi_k(a_0,y))dy\,. \qquad (1.21)$$

This solution does not explicitly include the control inputs or boundary condition information. In order to correct this problem, the approximation of the partial derivatives can be carried out including the control inputs and the boundary data. The distance h is step size between the points on the uniform Cartesian grid used for the finite-difference solution [4].

$$\frac{\partial}{\partial y}w(t,x,b_1)\approx u_{bottom}(t)\Psi_{bottom}(x)-w(t,x,b_1-h), \qquad (1.22)$$

$$\frac{\partial}{\partial y}w(t,x,b_2)\approx w(t,x,b_2+h)-u_{top}(t)\Psi_{top}(x), \qquad (1.23)$$

$$\frac{\partial}{\partial x} w(t, a_0, y) \approx \frac{w(t, a_0 + h, y) - f(h)}{h}, \tag{1.24}$$

After several substitutions, $w(t, x, y)$ can be approximated as a linear combination of POD modes when the α_k's are solved in the following system model. Then, the temporal model for the system is given by

$$\dot{\alpha} = A\alpha + Bu + N(\alpha) + F, \tag{1.25}$$

The matrix dimensions are then: A is N x N, B is N x 2, N and F are both N x 1.

The elements of the matrices A, B, N and F are of the following form, [4]

$$A(k, j) = -\frac{1}{h\,\mathrm{Re}} \begin{bmatrix} \int_{a_1}^{a_2} (\varphi_j(x, b_1 - h)\varphi_k(x, b_1) + \varphi_j(x, b_2 + h)\varphi_k(x, b_2))dx + \\ \int_{b_0}^{b_{end}} \varphi_j(a_0 + h, y)\varphi_k(a_0, y)dy + h\int_{\Omega} (\nabla\varphi_k(x, y) \bullet \nabla\varphi_j(x, y))dx \end{bmatrix}, \tag{1.26}$$

$$B = \frac{1}{h\,\mathrm{Re}} \begin{bmatrix} \int_{a_1}^{a_2} \varphi_1(x, b_1)\Psi_{bottom}(x)dx & \int_{a_1}^{a_2} \varphi_1(x, b_2)\Psi_{top}(x)dx \\ \vdots & \vdots \\ \int_{a_1}^{a_2} \varphi_N(x, b_1)\Psi_{bottom}(x)dx & \int_{a_1}^{a_2} \varphi_N(x, b_2)\Psi_{top}(x)dx \end{bmatrix}, \tag{1.27}$$

$$N(\alpha) = \frac{1}{2} \begin{bmatrix} \int_{\Omega} \left(\sum_{j=1}^{N} \alpha_j \varphi_j(x, y) \right)^2 \frac{\partial}{\partial x} \varphi_1(x, y)dx - \int_{b_0}^{b^{end}} \left(\sum_{j=1}^{N} \alpha_j \varphi_j(a_{end}, y) \right)^2 \varphi_1(a_{end}, y)dy \\ \vdots \\ \int_{\Omega} \left(\sum_{j=1}^{N} \alpha_j \varphi_j(x, y) \right)^2 \frac{\partial}{\partial x} \varphi_N(x, y)dx - \int_{b_0}^{b^{end}} \left(\sum_{j=1}^{N} \alpha_j \varphi_j(a_{end}, y) \right)^2 \varphi_N(a_{end}, y)dy \end{bmatrix}, \tag{1.28}$$

$$F = \begin{bmatrix} \int_{b_0}^{b_{end}} \left(\frac{1}{h\,\mathrm{Re}} f(y) + \frac{1}{2} f(y)^2 \right) \varphi_1(a_0, y) dy \\ \bullet \\ \bullet \\ \bullet \\ \int_{b_0}^{b_{end}} \left(\frac{1}{h\,\mathrm{Re}} f(y) + \frac{1}{2} f(y)^2 \right) \varphi_N(a_0, y) dy \end{bmatrix}. \qquad (1.29)$$

After the system of differential equations is solved for the α_k's, the resulting system approximation is finally known. The resulting $w(t, x, y)$ can then be compared with the original system response to verify the reliability of the reduced Galerkin model. Figure 5 gives a comparison between the full order finite-element based numerical solution and the 40 order nonlinear temporal model.

The value of the α_k's must be carefully projected onto the POD basis so that the two solutions will match. If this reduced POD model is shown to give consistent outputs to the full order system, it is possible to apply additional model reduction techniques. This reduced system can be used for simulation and control design.

Before the model reduction techniques can be performed on the nonlinear system, the realization must be linearized. We linearized the equations about the initial conditions as in [5]. The new state space and output equations are given by

$$\dot{\alpha}(t) = \widetilde{A}\alpha(t) + \widetilde{B}u(t), \quad \alpha(0) = \alpha_0 \qquad (1.30)$$

$$y(t) = \alpha(t) + \alpha(0) \qquad (1.31)$$

$$\widetilde{A} = \left. \frac{\partial(A\alpha + Bu(t) + N(\alpha) + F)}{\partial \alpha} \right|_{\alpha=\alpha_0} \qquad (1.32)$$

$$\widetilde{B} = \left. \frac{\partial(A\alpha + Bu(t) + N(\alpha) + F)}{\partial u} \right|_{u} \qquad (1.33)$$

However, since the partial derivative is taken with respect to u, $\widetilde{B} = B$.

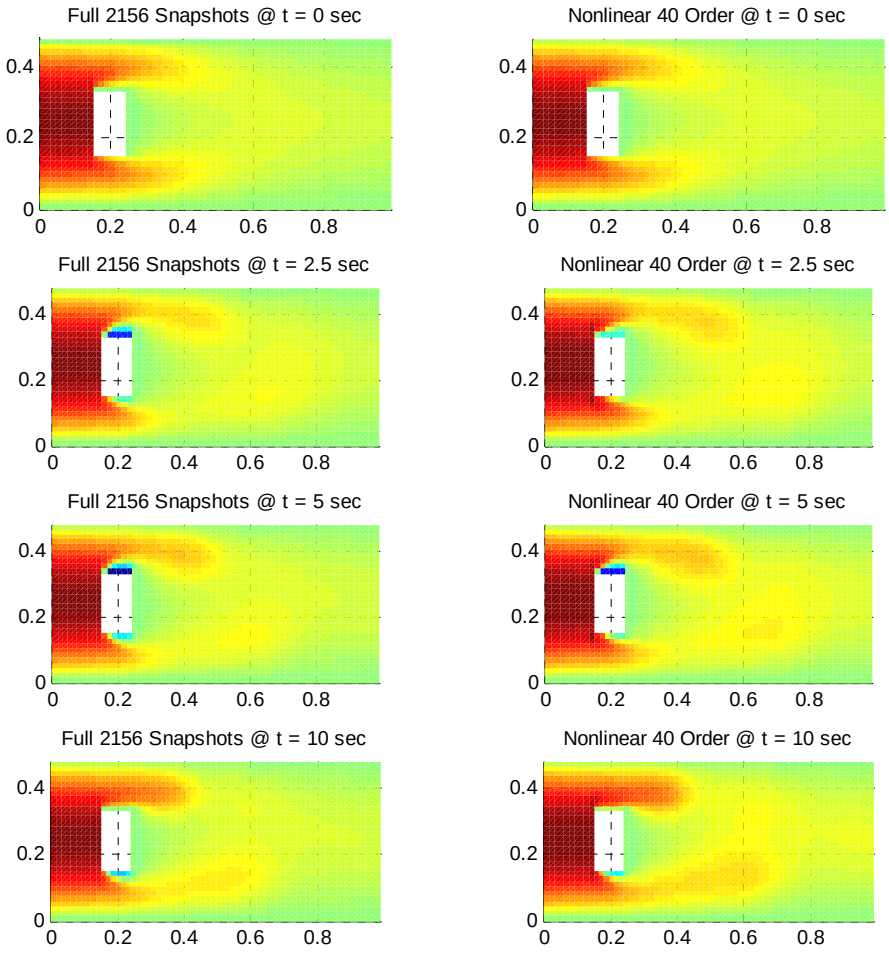


Figure 5. Comparison of 40-Order Galerkin Model and Full Order Snapshot Model Flow Solutions

Then, the linearized system described by (1.30) and (1.31) is available for using with conventional model reduction techniques. The important flow dynamics could be lost in the linearization process, which would make the resultant linear model a poor approximation to the 40^{th} order Galerkin model. However, to ensure that the linearized model will produce a similar flow, the flows of the two models must be compared.

The nonlinear 40^{th} order Galerkin model and the linearized 40^{th} order Galerkin model flows are compared in figure 6. The two flows show that the linearized model matches the nonlinear model very well.

Outline of the Thesis

This thesis looks at model reduction techniques for use with system models based upon nonlinear PDEs. In chapter II, we discuss some problems and considerations for system identification. Also we include an example of a simple system that does not have sufficient measurements to perform complete system identification. The chapter is concluded by brief descriptions of turbulence in fluid flows, the Navier-Stokes equations, Burgers equation, and computational fluid dynamics. Chapter III discusses model reduction methods: 'Design then Reduce' and 'Reduce before Design' and describes some of their characteristics. Further, we argue the benefits of a minimal realization. In chapter IV we discuss in detail the process of balanced truncation and Hankel optimal norm approximation model reduction.

Chapter V changes direction from the Galerkin weak model to empirically found realizations from simulation data. The Galerkin weak model is used to produce the outputs for use in the ERA method. First we test balanced truncation on an empirically created system realization. Then, we outline the process for the empirical balanced truncation model reduction technique.

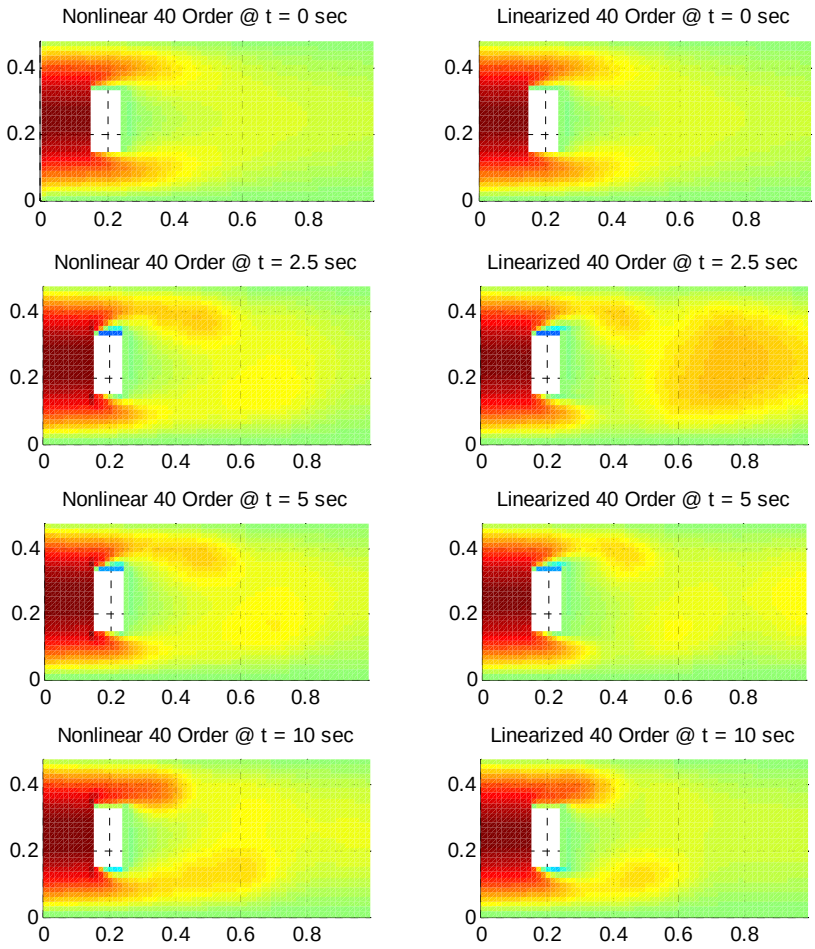


Figure 6. Nonlinear and Linearized Galerkin 40th Order Flow Solutions

Chapter VI includes the results from out model reduction efforts. A comparison between the Hankel optimal norm approximations, the standard balanced truncation method and the full-order nonlinear system model flows is made. Further, we present result from the empirically balancing truncation method. The chapter concludes with a comparison between the standard balanced truncation method and the empirically balanced truncation method. We include some discussion of the linear quadratic regulating control design procedure in chapter VII. Some simple results of control tracking are shown. Finally, in chapter VIII we give some conclusions about the relative effectiveness of the model reduction techniques and directions for future research.

CHAPTER II
BACKGROUND ON MODEL CREATION AND FLUID DYNAMICS

Real World Systems

Although the desire when creating a mathematical model of a process or device is for perfect accuracy, this feat is not possible. A perfect goal for a system model is that the system's true steady-state and dynamic response to all possible inputs and initial conditions are perfectly predicted by the model. Unfortunately, this is an unrealistic expectation for anything but the simplest of systems. A reasonable goal for a system model is to capture the "most important aspects" of the system or the process under consideration. The identity of the most important aspects will naturally be very different depending on the purpose of the model.

System Identification Preliminaries

The basic need for system identification comes from the desire to have a mathematical model that will predict the dynamic and steady state behavior of a real system. This mathematical model can then be used for system simulation or for controls design. There are many different methods for determining a mathematical model for a system. One common method is to use a physical understanding of the components of the system to produce a system of differential equations that describe the operation of the system. This method will often result in a system of coupled ordinary differential equations or a nonlinear partial differential equation (NPDE). The number of states needed for simulation of even simple NPDEs can easily reach thousands of states. Often, techniques from computational fluid dynamics are needed to solve these systems. For system simulation purposes in non-real time the solutions can certainly be calculated. However, the necessary computer computation power and simulation time might be prohibitively large. Conversely, control must usually be done in real-time, so the system model must be small enough that the control calculations can be performed in real-time.

Measurements

Measurements for system identification can be acquired in two broad ways. One way is through direct measurements from experimentation with a physical system. This method is both costly and time consuming. States can only be measured if an appropriate sensor is located in the system and captures the data. In general, it is not possible to excite the system such that every mode is activated [51]. In the case of PDE based system models it is impossible to excite every state since the number of states is infinite in these infinite dimensional system models. Ultimately, one would not want to risk harm to a real system to investigate possible unstable or uncontrollable states. Although blindly inserting inputs in an attempt to fully excite the system might lead to fallacious results, carefully selecting test inputs is a very practical and useful method. A very effective system model can be created by a system over a "standard operating range". The test inputs should include signals that typically are applied in the normal operation of the system [25]. Experimental results with the Caltech experiment for flexible structures show that valid system models are unable to always predict all the system parameters since mathematical models are only approximations of physical systems [17]. Then, empirical data can be used to produce the model's most important parameters. This is the reasoning that allows for the use of many system identification techniques such as the ERA, which is described in detail later for identifying the test system's Markov parameters.

The other primary method is to use mathematical models to simulate the operation of the system computationally. Then, the "measurements" are simply calculated values based upon one's best understanding of the system model *a priori*. The better the system's mathematical model, the more likely that a good computationally usable system model will be found. A very fortunate byproduct of using a computer simulation is that the time required for the identification is less important. A simulation for system identification can easily run on a computer

unattended. Additionally, there is no risk to the equipment or a person's safety from a case where the system goes unstable. Further one practical consideration is that system identification techniques must continue to excite the system with sufficient amounts of energy to keep the states excited to allow for measurements to be made. In theory, a frequency response based approach only needs an impulse response to appropriately excite the system for identification. However, in practice a random sequence signal of white noise or a varying sinusoidal input known as a squelch function is applied [25]. The idea of signal to noise ratio (SNR) explains why continuous excitation is needed in practice. The SNR is the ratio between the amplitudes of the signal that is being measured and the noise present with the signal. A single impulse only contains a large amount of energy for a single instant. This energy is quickly dissipated in a stable system. Accurate measurements can become very difficult to acquire when the SNR ratio becomes small. The true data and the error have approximately the same amplitudes, which results in no clear distinction between the data and the noise [53].

Model Interpretation

If an exact mathematical model is not available or is too complex to evaluate, one must rely on measured data to determine the system model. Some constraints on the model interpretation are unavoidable. Unobservable states by definition will not be detectable when measured from true system experimental data. The physical placement of sensors is very important since a sensor must be available for measuring a state (or an estimate of the state provided for by a state observer [20]) in order to record the given state value [52].

However, care must be taken to not inadvertently neglect unstable states simply because they are difficult to measure or are hidden by the initial test inputs to the system. Further, one pitfall that might be encountered is the failure to identify both a fundamental mode and one or more of its harmonics due to folding

frequencies [25]. Otherwise, very important system modes will remain completely unmodeled in the resulting system model. When using experimental data for a complex system, it is likely that the true system order will not be known. One will have to develop a model without knowing *a priori* the number of modes that ultimately will be needed. A reasonable and common practice uses special values of the system to see how important each state is in the input output behavior ([14], [33], [36]). The Hankel singular values, which are invariant to state transformations to quantitatively order the importance of the system input output behaviors. Accordingly, those lower valued Hankel singular values can be eliminated without loosing much of the system information. This idea leads to the model reduction techniques discussed later [39].

The accuracy and realism of a model is only as good as the criteria used to create the model. A simple example where the system model will definitely not provide the desired information can be seen in figure 7. The unicycle shown in figure 7 has an input in the form of a person or a circus bear pushing down on the pedals. The only sensor that has been placed on the system is a single 3-axis accelerometer. Although the accelerometer will determine the acceleration in 3 dimensions, the initial location, velocity, and acceleration of the wheel and the initial condition of the pedals are not known. However for full system identification, these initial conditions and more than a single sensor will definitely be needed. Additional states must be measured if the output for position is to be calculated. One sensor would be needed to track the position of the base of the wheel as the input is excited.

Moreover, without knowing the dimensions of the wheel or the gear to wheel ratio, the acceleration gives no information about the position of the unicycle. Although a little simplistic, this example shows that system identification can only be as good as the information that one is able to gather.

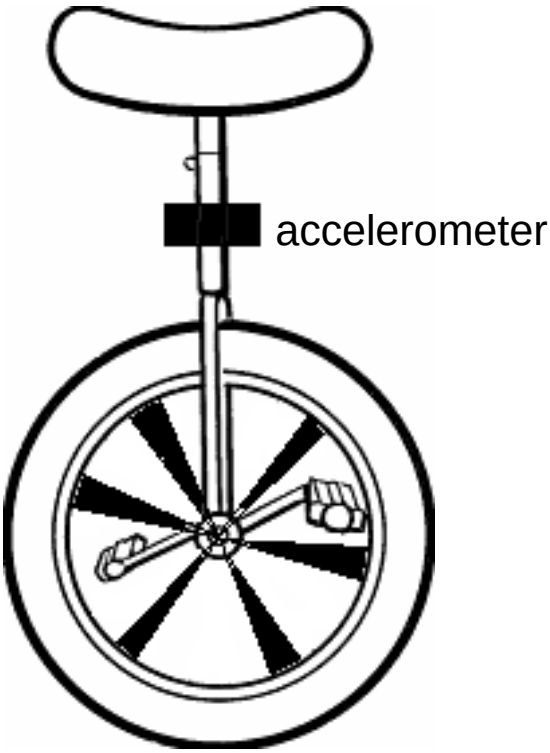


Figure 7. System with Insufficient Measurements for System Identification

There is another extreme to a system that is severely lacking necessary information to allow system identification. If a system could be fully understood from basic physics equations, then a perfect mathematical model could be developed. Unfortunately, a NPDE mathematical description that gives a near perfect description of the system's dynamic and steady state responses could be of very little use in the actual control design process. A system realization must be found so that standard control design techniques can be applied and so that the most important system dynamics are modeled well over the entire range of expected operation.

Fluid Dynamics Background

The application specifically considered in this thesis is fluid dynamical systems. Therefore, this section deals with some very basic background on fluid dynamics and the mathematics that commonly are used to describe its properties.

Turbulence

Turbulence is a common occurrence in almost all common fluid flows. Typically the idea of turbulence is considered to be a property of fluid flow. A precise definition of turbulence is difficult to give according to [26]. Therefore, when turbulence is described the characteristics of turbulence are often given. These characteristics include randomness, 'diffusivity', and the fact that all turbulent flows are dissipative. In this case randomness describes the chaotic behavior of the flow. 'Diffusivity' is the characteristic of turbulence that allows for rapid transportation of energy to surrounding particles and it causes rapid mixing and fuels the increase of momentum, heat, and mass transfer [26]. A crude example of how this property is important is an uninsulated steam line versus a space heater. The steam line might have a very high surface temperature but if there is very little air movement in the room, the air temperature on the other side of the room will change slowly. However, if a space heater is turned on the air temperature in the entire room will increase much more rapidly. The property of

dissipation results from shear stresses that help to deform the flow's shape and result in reduced internal kinetic energy [26]. Eventually the losses will overcome the driving force, and the flow will be dissipated.

The Reynolds number is a very important number in fluid dynamics because it gives some vital information about the flow. A flow however does not have a single Reynolds number, but many usually related Reynolds numbers. In general a specific Reynolds number is determined by a fluid's velocity times the length in question divided by the kinematic viscosity. Flows having a low Reynolds' number are typically considered laminar in nature. Solving fluid equations that are laminar is quite straightforward and can be simplified from the PDE form without much loss of accuracy. Those flows that have high Reynolds numbers, a distinction that varies with geometry, display turbulent flow. Unfortunately, solving turbulent flows involves the solution to a complex Nonlinear PDE that must be supplemented with "closure relations" [26].

Navier-Stokes Equations

The Navier-Stokes Equations are used to describe fluid flow in n-dimensions. This equation is a nonlinear partial differential equation (NPDE) that at this time has no known exact solution for the general case [21]. Given the initial conditions and the external forcing function, the equations are to be solved to find the velocity of the fluid, as well as the pressure if the fluid is a gas, at any point and time within the problem boundary. A general closed-form solution to the Navier-Stokes equations would essentially be the solution to turbulence [26]. The term u is the velocity of a particle in the fluid at a specific time and point in space. Further, p is the fluid's corresponding pressure at that same point and time. The standard Navier-Stokes equations for a compressible fluid has the form [21]

$$u_t - v\Delta u + u \bullet \nabla u + \nabla p = f \tag{1.34}$$

$$u\big|_{\partial\Omega} = 0,\ u(0) = u_0\,. \tag{1.35}$$

The first equation, momentum conservation, expresses the balance of forces on the left hand side (lhs) summing to the applied external force f. The boundary condition given in equation (1.35) means that if $\partial\Omega \neq \varnothing$ then $u(t,x) = 0$ holds for all $t \in [0,T)$ and $x \in \partial\Omega$ [21]. Since this equation is multi-dimensional, the derivative of $u_t = \frac{\partial}{\partial t}u$ and the total acceleration for a given particle in the fluid flow is given by [21]

$$u_t + u \bullet \nabla u = u_t + \left(\sum_{i=1}^{n} u_i \frac{\partial}{\partial x_i} \right) u \,. \tag{1.36}$$

The friction between the individual particles in the fluid flow is described by [21]

$$-v\Delta u = -v\left(\sum_{i=1}^{n} \frac{\partial^2}{\partial x_i^2} \right) u \,. \tag{1.37}$$

The final term of the first term is the gradient of the pressure. The general solution to the full nonlinear Navier-Stokes equations has yet to be found. One claim for a general solution by Hui-chuan [11] proposes exact solutions to a slightly simpler form of this equation that uses the theory of functions of a complex variable with a Dirac-Pauli representation. Further, the Navier-Stokes equations are turned into a nonlinear equation containing two complex unknown functions. However, the method eventually reduces the Navier-Stokes Equations to a form of the Burgers Equation. Therefore, this solution is not general, but might be a gateway to finding a general closed solution.

Burger's Equation

Often, a simpler PDE is used to approximate the flows in fluid dynamics ([4], [5], [15], [24]). The Burger's equation has a nonlinearity similar to the Navier-Stokes equations and is a good test equation for developing controls for fluid dynamic systems [24]. The equation that is specifically considered in this thesis is the two-dimensional Burger's equation [4].

$$\frac{\partial}{\partial t} w(t,x,y) + \nabla \bullet F(w) = \frac{1}{r}\left(\frac{\partial^2}{\partial x^2} w(t,x,y) + \frac{\partial^2}{\partial y^2} w(t,x,y) \right) \tag{1.38}$$

where the form of F(w) is

$$F(w) = \left[c_1 \frac{w^2(t,x,y)}{2} \qquad c_2 \frac{w^2(t,x,y)}{2} \right]^T . \tag{1.39}$$

The value r can be used to simulate the effect of the Reynold's number in the Navier-Stokes equations. The terms c_1 and c_2 are nonnegative constants that are application specific. The function $w(t,x,y)$ describes the velocity of a given particle in a fluid flow. Several papers ([4], [5], [15], [24]) use Burger's equation as a surrogate to the Navier-Stokes Equation in order to test concepts of model reduction.

Computational Fluid Dynamics

For many applications this classic method is used for solving PDEs. Computational fluid dynamics (CFD) is a numeric method for solving fluids and heat transfer problems. Finite difference methods have historically been the primary method used in the CFD community [13]. The original system model for our problem geometry, as developed in [4], uses this well known method. The method is based upon the idea of using finite difference equations to approximate the value of the derivative of the equation [13].

The basic idea of finite element analysis involves using structured or unstructured meshes in the appropriate number of dimensions to discretize the region into finite elements. [35]. The mesh number and geometry is a design decision. A greater number of elements will often improve the reliability of the solution but requires a longer time to solve the equation and greater memory requirements. This solution method is widely known and is available as a toolbox for Mathwork's popular product Matlab [18]. Complex nonlinear PDEs in most cases cannot be solved directly. Generally closed form solutions for these types of equations are open problems in research. If closed solutions are found for these types of problems they often require very specific boundary conditions in order to obtain the solution. If a closed solution is not known for the PDE with the

specific boundary conditions that apply, a different method than direct evaluation is absolutely necessary. Therefore, effective numerical methods are important for implementing a solution method quickly in computers. In practice, this usually means that a CFD model is created and solved. Unfortunately, the time needed for these calculations can be quite large.

CHAPTER III
MODEL REDUCTION

Model Reduction Approaches

As with most things where the tradeoffs between two alternatives can be quite significant, there is difference of opinion on the basic methodology of model reduction. There are two major philosophies of how to accomplish closed loop control design using model reduction techniques. These two philosophies are referred to in literature [1], [15], as the ‘Reduce before Design’ and the ‘Design then Reduce’ methods. The basic path for each of these model reduction ideals is depicted in Figure 8. There are positives and negatives to both of the philosophies that ultimately dictate which is more appropriate or reasonable for use in a specific application.

The ‘Design then Reduce’ approach has the benefit that the reduced order controller is created using information from the full order system model. Therefore, the closed-loop system with the reduced order controller can be simulated to verify that all the important system dynamics are controlled. Another benefit of this method is that it is potentially a problem to discard full system information before the control design occurs [47]. A negative of this method is that the computational requirements of the ‘Design then Reduce’ can be very large if the original system model contains many states. The approach of ‘Design then Reduce’ has been successfully applied for some systems described by partial differential equations (PDE)s ([1], [48], [49]). The design of low order controls is important for very large-scale systems of ordinary differential equations (ODE) [1]. The computation time and memory use for calculating large systems of ODEs can be prohibitively large for real-time control in embedded systems. However, low order control is absolutely necessary for real-time control of systems described by complex PDEs.

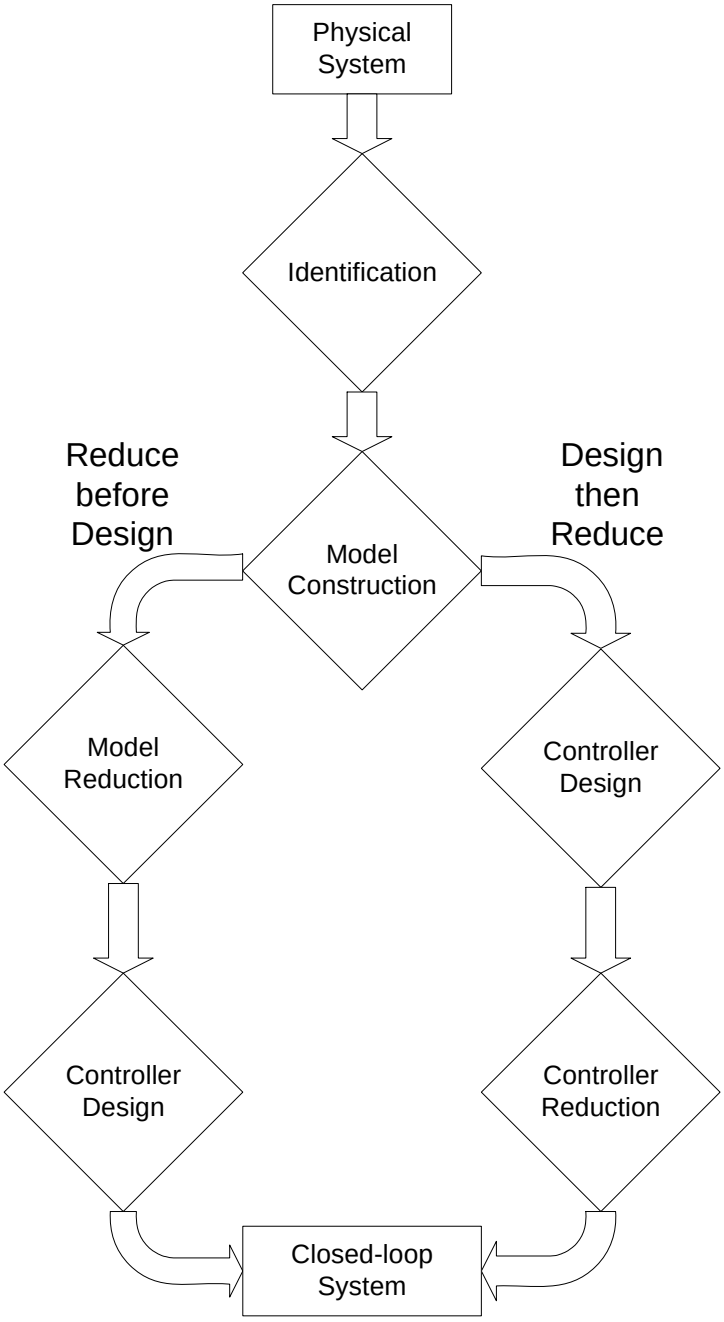


Figure 8. Model Reduction Paths

The computation time and memory use for the solution of complex PDEs is huge. The computational needs to find a solution to a complex PDE make the solution to large systems of ODEs seem trivial by comparison. Typically the approach for control synthesis when the original system model is in the form of a PDE is to use the “reduce-before-design” path and then to use standard control designs such as linear-quadratic Gaussian (LQG), min-max, or H_∞ [1]. This strategy allows the use of existing computational and control design techniques. Further, this approach is useful for simulation purposes because it makes the system model much easier to quickly evaluate for various values [1]. However, there is one major problem with the ‘Reduce before Design’ method. When, the system model is reduced, there is a chance that some important system dynamics could be lost. One important thing to keep in perspective is that model reduction is an approximation of the mathematical representation of the system. The reduced order controller will be applied to the physical system. Consequentially, control design must be robust enough to provide the desired output without having full system dynamics information. The states that are truncated from the mathematical model remain in the original physical system. If proper model reduction has been performed, the contribution of the un-modeled states to the output(s) should be minimal.

Various methods for the creation of the system model are used in practice ([3], [7], [8], [12], [14], [27], [36]). These methods are used as tools to get an initial model or to create a model of usable size. Each has its own strengths and is appropriate to use in certain cases. If a reasonably accurate model is obtained, the models can be reduced further using standard model reduction techniques.

Simplicity and Accuracy

The basic tradeoffs between accuracy and simplicity are encountered in model reduction. Control design using conventional methods is much simpler with a

realization including only a small number of states than with a realization that is not minimal and has thousands of states.

A minimal realization can be a very effective tool in control design. There are an infinite number of valid realizations for a system. As the name suggests, a minimal realization for a system is one whose state space has the smallest possible size. However, since the system realization will be used to calculate the control law, the speed of computation and the resulting computational cost is very important. The speed of computation is directly dependant upon the size of the matrices being multiplied. A minimal realization is then a very beneficial arrangement of the system information from a practical computational sense. Finding a minimal realization starts with a valid state-space system realization with no condition placed on its stability [6]. After a minimal realization has been found for the system, an informed model reduction process can be started. The elimination of uncontrollable and unobservable states is an important first step in model reduction. In the context of model reduction, the first states to be eliminated should be those that do not contribute to the input-output relationship of the system. These uncontrollable and unobservable states are not necessary in the system model; thus they should be the first states to be eliminated. Since all the uncontrollable and unobservable states have been eliminated, a minimal realization gives the benefit of full state observability and controllability [22]. System dynamics simulations and control design using computers is much faster when the matrices being used have small dimensions. Unfortunately, some of the system dynamics might be completely lost if too many states are eliminated.

Conversely, a system with a million states cannot be solved with current computers. This illustrates that with the tradeoffs between simplicity and accuracy there is a need for optimal model reduction techniques that can give the benefit of a reduced size system realization while maintaining sufficient information to accurately capture the system dynamics.

CHAPTER IV
MODEL REDUCTION USING BALANCED TRUNCATION AND HANKEL NORM APPROXIMATION

The model reduction techniques used with the Galerkin model calculated from the POD basis were balanced truncation and Hankel optimal norm approximation to further reduce the approximation of equation (1.25).

Balanced Truncation

Some basic understanding of realizations is necessary before balanced truncation can be discussed. A realization of a time invariant continuous (in time) system is the following continuous time state space model

$$\begin{aligned} \dot{x}(t) &= Ax(t) + Bu(t), \\ y(t) &= Cx(t) + Du(t). \end{aligned} \tag{4.1}$$

The first equation gives the value for the states of the system, $x(t)$. The state vector $x(t)$ is a column vector that is conformable with the *n* x *n* state matrix A and is composed of all the system states. The matrix A is known as the state matrix because it describes the linear combination of the states. The input matrix, B, describes how the inputs are combined and scaled in the system dynamics. The second equation is the output equation that gives the output, $y(t)$, of the system as the sum of the output matrix C times the state values and the feed forward matrix D times the current inputs. The matrix C describes how the states are scaled and coupled in the output. Finally, the matrix D describes the linear combination of the current inputs that appear in the current output.

Further, in a very similar manner the realization of a discrete time system is the following discrete time state space model

$$\begin{aligned} x(k+1) &= Ax(k) + Bu(k), \\ y(k) &= Cx(k) + Du(k); \end{aligned} \tag{4.2}$$

where the values for k correspond to the samples of the input and output.

The realization of the system is typically defined as finding the triplet of the A, B, and C matrices [25]. Usually the D matrix is not considered as part of the realization, since the vast majority of systems are proper and it does not affect the states.

A system in general has an infinite number of realizations. In the case of multivariable systems it becomes very likely that a realization formed by standard methods will not be a minimal realization [20]. Each of the inputs and outputs has a realization, which together make up the total system realization. Let each of the realization elements be of the form

$$G_i(s) = \left[\begin{array}{c|c} A_i & B_i \\ \hline C_i & D_i \end{array}\right]. \tag{4.3}$$

This equation might be misleading. Equation (4.3) is a standard notational tool use in many controls textbooks [6], [22], and [23]. The rhs is actually the state space representation of the transfer function $G_i(s)$ on the lhs. Then, with an example having $G_1(s)$ and $G_2(s)$ the overall system can be factored into the following form

$$G(s) = \left[\begin{array}{cc|cc} A_1 & \bar{0} & B_1 & \bar{0} \\ \bar{0} & A_2 & \bar{0} & B_2 \\ \hline C_1 & C_2 & D_1 & D_2 \end{array}\right] \tag{4.4}$$

where A_i, B_i, C_i, and D_i for $i \in \{1,2\}$ are matrices. A representation of the system given by the realization in (4.4) is shown in figure 9.

If this realization (4.4) is stable, the minimal realization can then be found using method involving the controllability and observability Gramians. This method is described in detail in [23] and [20]. The procedure of balanced truncation starts with the creation of the controllability and observability Gramians of a stable system.

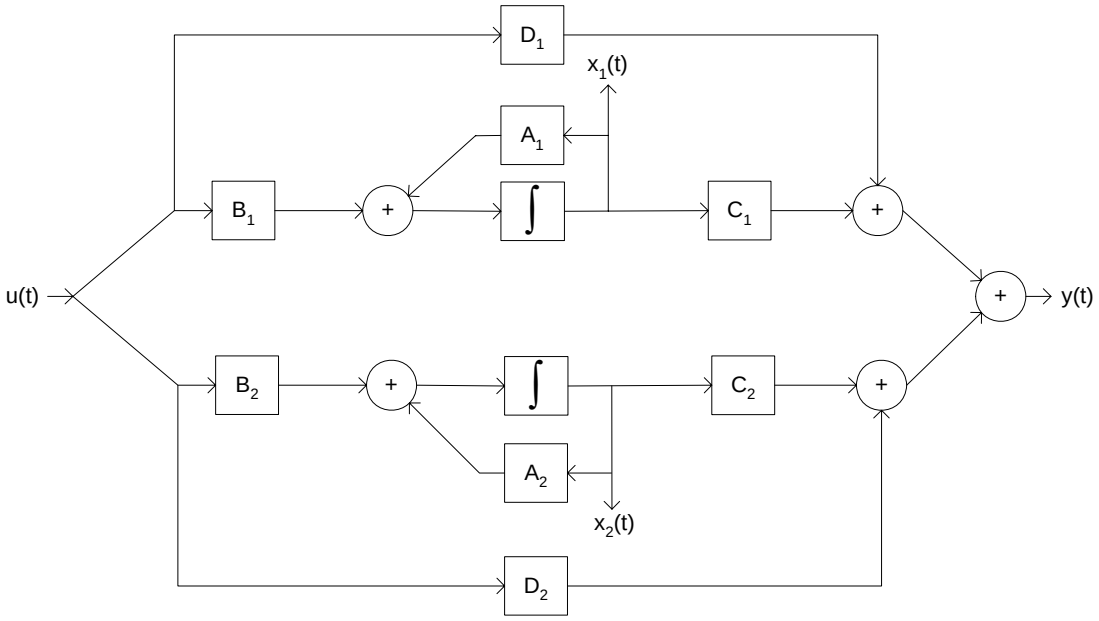


Figure 9. State Space Realization Separating Inputs

The controllability and observability Gramians are given by the following equations.

$$W_c(t) := \int_0^t e^{A\tau} BB^* e^{A^*\tau} d\tau \; ; \tag{4.5}$$

$$W_o(t) := \int_0^t e^{A^*\tau} C^* C e^{A\tau} d\tau \; . \tag{4.6}$$

The Lyapunov equations can be used to find a solution to these Gramians for the time-invariant case if the system matrix A is stable [6].

$$A^* X + XA + Q = 0 \; ; \tag{4.7}$$

$$AX + XA^* + Q = 0 \; . \tag{4.8}$$

The unique solution for X for the time-invariant case, with the square matrices A and Q and where A is Hurwitz and stable, as shown in [6], is

$$X = \int_0^\infty e^{A^*\tau} Q e^{A\tau} d\tau \; . \tag{4.9}$$

This is an analogous equation to the controllability and observability Gramians with Q replaced by BB^* and C^*C respectively. Then, the Lyapunov equations

needed for solving the controllability and observability Gramians for the time-invariant case if the system matrix A is stable become

$$AW_c + W_c A^* + BB^* = 0 \tag{4.10}$$

$$A^* W_o + W_o A + C^* C = 0 \tag{4.11}$$

Although not necessary, finding a minimal realization before the balanced truncation method is a reasonable and good practice to follow [39]. Since the goal of model reduction is to reduce the number of states necessary to form a reliable system model, a minimal realization is desirable to have before forming a balanced realization.

The definition of a minimal realization is a state space realization that has an A matrix with the smallest possible dimension. Although this is the definition, a test is needed to see if a particular realization meets this criterion. A necessary and sufficient condition is that the controllability matrix (A, B) is controllable and the observability matrix (C, A) is observable where

$$(C, A) = \begin{bmatrix} C \\ CA \\ CA^2 \\ \vdots \\ CA^{n-1} \end{bmatrix}; \tag{4.12}$$

$$(A, B) = \begin{bmatrix} B & AB & A^2 B & \cdots & A^{n-1} B \end{bmatrix}. \tag{4.13}$$

The state space given as equation (4.1) is controllable over the time period $\left[t_0, t_f\right], t_f > t_0$ if for any initial state $x(t_0) = x_0$ there is a continuous input signal $u(t)$ such that the solution of (4.1) will satisfy $x(t_f) = 0$ [20]. The state space given as equation (4.1) is observable on $\left[t_0, t_f\right], t_f > t_0$ if any initial state $x(t_0) = x_0$ is uniquely determined by a specific $y(t)$ where $t \in \left[t_0, t_f\right]$ [20]. The test for

controllability and observability can be performed in the following way. Compare the rank of (A, B) and the rank of A. A fully controllable realization will produce a controllability matrix that has the same rank as the state matrix A. Compare the rank of (C, A) and the rank of A. A fully observable realization will produce an observability matrix that has the same rank as the state matrix A.

Very important results from [39] show that the controllability and observability Gramians contain “second order modes” that invariant to transformations. A balanced realization seeks to balance the observability and controllability of the system. Therefore each of the states in the balanced state will just as controllable as it is observable. Ultimately a balanced realization (or internally balanced realization) needs a similarity transformation such that

$$\hat{W}_0 = \Sigma = \hat{W}_c \tag{4.14}$$

where the matrix Σ is a diagonal matrix containing constants in monotonically decreasing order. The elements of this matrix’s diagonal are known as the Hankel singular values of the system. The controllability and observability Gramians will then be equal and diagonal. To get to this balanced realization some steps need to be followed. Start the balancing process with a stable minimal realization system G where

$$G = \left[\begin{array}{c|c} A & B \\ \hline C & D \end{array}\right]. \tag{4.15}$$

Note that no restriction is placed on continuous time or discrete time in equation (4.15). The following process will work identically the same for both a continuous time and a discrete time state space representation.

First find a matrix R that satisfies

$$W_c = R^* R. \tag{4.16}$$

Then diagonalize the matrix RW_oR^* according to

$$RW_oR^* = U\Sigma^2U^* \tag{4.17}$$

where U is a unitary matrix. Then, the needed transformation matrix to balance the controllability and observability Gramians is given by

$$T^{-1} = R^{*}U\Sigma^{-1/2}. \tag{4.18}$$

The balanced Gramians become

$$TW_cT^{*} = (T^{*})^{-1}W_oT^{-1} = \Sigma \tag{4.19}$$

where

$$\Sigma = diag\left(\sigma_1,\ \sigma_2,\ \ldots,\ \sigma_n\right). \tag{4.20}$$

This equation then shows the relationship between W_c and $\widehat{W_c}$ and W_o and $\widehat{W_o}$ when taken together with equation (4.14). The diagonal matrix Σ contains the Hankel singular values of the system. When the states are transformed by the T matrix, the new states are related to the original states such that,

$$\hat{x} = Tx \tag{4.21}$$

And the resulting system realization becomes

$$G = \left[\begin{array}{c|c} \hat{A} & \hat{B} \\ \hline \hat{C} & \hat{D} \end{array}\right] = \left[\begin{array}{c|c} TAT^{-1} & TB \\ \hline CT^{-1} & D \end{array}\right]. \tag{4.22}$$

This system is a balanced realization that shows the relative importance of the input output pairs. Finally the controllability and observability Gramians become

$$\widehat{W_c} = TW_cT^{*}, \tag{4.23}$$

$$\widehat{W_o} = (T^{-1})^{*}W_oT^{-1}, \tag{4.24}$$

where the pair $\widehat{W_c}$ and W_c have different eigenvalues. Additionally, the pair $\widehat{W}_c$ and W_c have different eigenvalues. However, the eigenvalues of the product of the two Gramians are invariant to the transformation matrix T.

$$\widehat{W_c}\widehat{W_o} = TW_cW_oT^{-1}. \tag{4.25}$$

The positive square roots of the eigenvalues of the above product are known as the Hankel singular values (HSV) of the system. The value of the positive square roots of the left hand side and the right hand side are equal [23].

Then, the all-important Hankel singular values have been found. Since the Hankel singular values relate the relative importance of the input-output relationships some of the less important values can be truncated without loss of much information [33]. Small Hankel singular values correspond to weakly controllable and weakly observable states [39]. The basic claim of the balanced truncation method is that the overall quality of the model will not be degraded much by eliminating states that are not very observable or controllable [39]. An upper bound on the error is given by equation (4.29).

A suitable tolerance below which HSV are considered irrelevant should be chosen. Then, the diagonalized balanced Gramians should be partitioned in the following way [22]

$$\Sigma = \begin{bmatrix} \Sigma_1 & 0 \\ 0 & \Sigma_2 \end{bmatrix}. \tag{4.26}$$

Where the Gramians remain equal and balanced. Σ_2 holds those HSVs that have smaller numeric values than the previously chosen tolerance.

If the balanced realization is partitioned as [22]

$$G = \left[\begin{array}{cc|c} A_{11} & A_{12} & B_1 \\ A_{21} & A_{22} & B_2 \\ \hline C_1 & C_2 & D \end{array}\right], \tag{4.27}$$

the Gramians are balanced and equal. However, since the Gramians are diagonal, a portion of the main diagonal is associated with A_{11} and the remaining portion of the diagonal to associate with A_{22}. The value for all of the HSVs less than a prescribed tolerance can be forced to identically equal 0.
Therefore, the resulting system becomes [22]

$$G_{r_k} = \left[\begin{array}{c|c} A_{11} & B_1 \\ \hline C_1 & D \end{array}\right] \tag{4.28}$$

where A_{11} is square and of size k x k. Now, the original system has first been given a minimal realization, then the minimal realization balanced so that the controllability and observability Gramians are equal and diagonal. Finally, the system has been truncated subject to the desired number of HSVs to keep.

The error bounds for balanced truncation can be expressed in the following manner [23] and [6].

$$\left\| G(s) - G_{r_k}(s) \right\|_\infty \le 2\left(\sigma_{k+1} + \sigma_{k+2} + \ldots + \sigma_n\right) \tag{4.29}$$

This bound on the norm allows the designer to have information about how much "change" will be encountered before the reduction. Although the bound is only on the infinity norm, it does give some insight into when the magnitude of the next truncated HSV will start to have a major impact on the overall "closeness" to the original system.

Hankel Optimal Norm Model Reduction

The Hankel optimal norm model reduction approximation was first applied for the purpose of model reduction by Kung [50]. First the optimal solution was found for scalar systems and then multivariable systems in [45] and [46] respectively. Significant advances to this model reduction technique came in [9]. Glover used state space system representations and provided an upper bound on the error in terms of the L_∞ norm. Hankel optimal norm model reduction starts with an understanding of the Hankel operator. Recall that if a system is given by $G(s)$ then $g(t)$ is its inverse Laplace transform, which is also the system's impulse response. The Hankel operator is defined in the time domain as [22]

$$\Gamma_g : L_2(-\infty, 0] \mapsto L_2[0, \infty). \tag{4.30}$$

given a function $f \in L_2(-\infty, 0)$

$$\Gamma_g f := P_+(g * f) \tag{4.31}$$

where the operator P_+ is defined in the time domain as

$$P_+ : L_2(-\infty, \infty) \mapsto L_2[0, \infty). \tag{4.32}$$

Equation (4.31) gives the result that when the Hankel operator is applied to the function f, the causal impulse response of the system is given. The Hankel operator when applied to the state-space model is finite-rank. The dimension of the range is finite and equal to the number of states in the temporal model. Suppose a stable G with state space realization as given by (4.1), then in the time domain

$$\Gamma_g u(t) = \int_{-\infty}^{0} Ce^{A(t-\tau)} Bu(\tau) d\tau, \quad t \geq 0, \tag{4.33}$$

which can be written as

$$y(t) = \Gamma_g u(t), \quad t \geq 0. \tag{4.34}$$

The interpretation of the Hankel operator to state space representation is a map from past inputs to future outputs [22]. Two other important operators play a role: the controllability operator and observability operator. These operators are defined such that

$$\Psi_c : L_2(-\infty, 0] \mapsto \mathbb{C}^n; \tag{4.35}$$

$$\Psi_c u := \int_{-\infty}^{0} e^{-A\tau} Bu(\tau) d\tau \tag{4.36}$$

$$\Psi_o : \mathbb{C}^n \mapsto L_2[0, \infty]. \tag{4.37}$$

$$\Psi_0 x_0 := Ce^{At} x_0, \quad t \geq 0 \tag{4.38}$$

The controllability operator maps past inputs to the current values (initial conditions). The observability operator maps the initial conditions to the future inputs. These operators can be thought of as the two intermediate steps of the Hankel operator such that the Hankel operator can be interpreted as

$$\Gamma_g = \Psi_c \Psi_o. \tag{4.39}$$

Equation (4.39) shows that there is a close relationship between the observability and controllability of the system states and the Hankel operator acting on the system.

The Hankel optimal norm approximation tries to find a new system realization given by

$$\dot{\tilde{x}}(t) = A_r \tilde{x}(t) + B_r u(t) \tag{4.40}$$

$$\tilde{y}(t) = C_r \tilde{x}(t) \tag{4.41}$$

where $\tilde{x}(t)$ is a different set of states based upon the new system realization. The triplet (A_r, B_r, C_r) is then the realization of $\hat{G}(s)$ that corresponds to the optimal Hankel norm approximation that has rank k strictly less than n.

$$\inf_{\substack{\hat{G}\in H_\infty \\ rank=k}} \left\| G(s) - \hat{G}(s) \right\|_H = \left\| G(s) - G_r(s) \right\|_H \tag{4.42}$$

where the rank of $G_r(s)$ is equal to k < n. The Hankel norm is given by

$$\left\| G \right\|_H = \left\| \Gamma_G \right\| = \sup_{\substack{u\in L^2(-\infty,\infty) \\ \|u\|_2 \le 1}} \left\| \Gamma_G u \right\|_2 . \tag{4.43}$$

The optimal Hankel norm approximation needs to first consider an all-pass transfer function. The computation uses an all-pass dilation to analyze the error between the system and the approximation to the system. The process has several steps that must all be completed to find the optimal Hankel norm approximation.

Again, start with a system transfer function of the form

$$G(s) = \left[\begin{array}{c|c} A & B \\ \hline C & D \end{array}\right] \tag{4.44}$$

with A, B, C, and D mutually conformable and capable of being converted to a balanced realization. Next, return to the Lyapanov equations to solve for the controllability and observability Gramians. Then, form a balanced realization with

$$A = \begin{bmatrix} A_{11} & A_{12} \\ A_{21} & A_{22} \end{bmatrix}, \quad B = \begin{bmatrix} B_1 \\ B_2 \end{bmatrix}, \quad C = \begin{bmatrix} C_1 & C_2 \end{bmatrix}. \tag{4.45}$$

The balanced Gramians given by Σ can be partitioned as

$$\Sigma = \begin{bmatrix} \Sigma_1 & 0 \\ 0 & \Sigma_2 \end{bmatrix} \tag{4.46}$$

Next, two special matrices need to be defined. A unitary matrix U must be found that holds for

$$B_2 = -C_2^* U \,. \tag{4.47}$$

Further [22],

$$\Gamma = \Sigma_1 \Sigma_2 - \sigma^2 I \,, \tag{4.48}$$

where $\sigma^2 \neq 0$ is an eigenvalue of $\Gamma_g^* \Gamma_g$. Then, define a special realization [22]

$$W(s) := \left[\begin{array}{c|c} \widehat{A} & \widehat{B} \\ \hline \widehat{C} & \widehat{D} \end{array}\right] \tag{4.49}$$

with the components given by the following [22]

$$\widehat{A} = \Gamma^{-1}(\sigma^2 A_{11}^* + \Sigma_2 A_{11} \Sigma_1 - \sigma C_1^* U B_1^*) \tag{4.50}$$

$$\widehat{B} = \Gamma^{-1}(\Sigma_2 B_1 + \sigma C_1^* U) \tag{4.51}$$

$$\widehat{C} = C_1 \Sigma_1 + \sigma U B_1^* \tag{4.52}$$

$$\widehat{D} = D - \sigma U \,. \tag{4.53}$$

The error between the transfer function $G(s)$ and the special realization $W(s)$ can be thought of as a transfer function of its own. This error transfer function is

$$E(s) = G(s) - W(s) = \left[\begin{array}{c|c} A_e & B_e \\ \hline C_e & D_e \end{array}\right] \tag{4.54}$$

where

$$A_e = \begin{bmatrix} A & 0 \\ 0 & \widehat{A} \end{bmatrix}, \quad B_e = \begin{bmatrix} B \\ \widehat{B} \end{bmatrix}, \quad C_e = \begin{bmatrix} C & -\widehat{C} \end{bmatrix}, \quad D_e = D - \widehat{D} \,. \tag{4.55}$$

Now that the transfer function has been transferred to an all-pass dilatation form, the process to find the optimal Hankel norm approximation can actually start. If the transfer function $G(s)$ is stable and square then the following holds [22]

$$\sigma_{k+1} = \inf_{\widehat{G} \in H_\infty} \left\| G(s) - \widehat{G}(s) \right\|_H = \inf_{\widehat{G} \in H_\infty, F \in H_\infty^-} \left\| G(s) - \widehat{G}(s) - F(s) \right\|_\infty \tag{4.56}$$

where the McMillan degree of the approximated transfer function is $\leq k$ [22]. The McMillan degree is the highest power of s in the denominator of the individual elements of a multivariable transfer function $G(s)$. H_∞ is the Banach space of L_∞ functions that are analytic in the right half plane and H_∞^- is the Banach space of L_∞ functions that are analytic in the left half plane. Then, if $G(s)$ has HSVs:

$$\Sigma = diag(\sigma_1, \sigma_2, \cdots \sigma_k, \sigma_{k+r+1}, \cdots \sigma_n, \sigma_{k+1}, \cdots, \sigma_{k+r}) \tag{4.57}$$

$\widehat{G}(s)$ is the optimal Hankel norm approximation iff there exists a $F(s) \in H_\infty^-$ that has a McMillan degree less than or equal to $n+k$ -1, and the error function

$$E(s) := G(s) - \widehat{G}(s) - F(s) \tag{4.58}$$

satisfies the constraint

$$E(s)E^T(-s) = \sigma_{k+1}^2 I \tag{4.59}$$

Then, the optimal Hankel norm approximation is given by $\widehat{G}(s)$ where

$$\widehat{G}(s) + F(s) = \left[\begin{array}{c|c} \widehat{A} & \widehat{B} \\ \hline \widehat{C} & \widehat{D} \end{array}\right]. \tag{4.60}$$

Since the Hankel optimal norm approximation is included in the preceding equation, it can be explicitly found if the value for $F(s)$ is found.

Then, the bound on the error gives that the

$$\inf_{\widehat{G}} \left\| G(s) - \widehat{G}(s) \right\|_H \geq \sigma_{k+1}(G(s)); \tag{4.61}$$

and the upper bound in terms of the L_∞ norm is given by

$$\left\| G(s) - G_r(s) \right\|_\infty \leq \left(\sigma_{r+1} + \sigma_{r+2} + \ldots + \sigma_n \right) \tag{4.62}$$

CHAPTER V
FREQUENCY DOMAIN REALIZATION TECHNIQUES

Empirical Realization Methods

Several frequency domain identification techniques are used in practice. One such method that is a well-defined frequency domain system identification is the Eigensystem Realization Algorithm (ERA) technique [25]. Unlike the POD method, the ERA based system realization model is created directly from empirical data and frequency domain characteristics of transfer functions. One very effective method for finding important information about a system directly from experimental data is using a frequency domain method to find the Markov parameters of the system. This method is applied to discrete time versions of system models.

The ERA and the empirical balancing method are discussed, which are used in many cases ([3], [14], [15], [27]) to identify the system based upon experimental or simulated results. The basic idea is to form an approximated empirically obtained system realization (the matrices $\hat{A}, \hat{B},$ and $\hat{C}$) from the system's Markov parameters or the approximated empirically found controllability and observability Gramians from system input output behavior. The workhorse of the method involves finding the system Markov parameters to populate a matrix that gives the impulse response from each input to each output at various time steps. The Markov parameters for a known system are of the following form

$$Y(0) = D,\ Y(1) = CB,\ Y(2) = CAB,\ \cdots,\ Y(k) = CA^{k-1}B \tag{5.1}$$

The importance of the ERA method can quickly be appreciated when one thinks about a system that does not have a well-defined mathematical description. Then, the choice of how to proceed in the control design process becomes: develop a mathematical model of extreme quality or develop an empirical model

that uses actual experimental data to develop the system realization. From a practical sense the empirically obtained model will be an easy choice.

The empirical balancing method is explored in [9]. The controllability and observability Gramians for nonlinear systems cannot be found in general. Since the Gramians cannot be found explicitly, the system balancing transformation cannot be found either. Empirical data can be used to find an approximate set of controllability and observability Gramians, which can be used to find a system balancing transformation. Therefore, if a balancing transformation can be found from the empirical data, the same balancing transformation can be applied to the original system. A more complete description of the mathematics of the balanced realization is found in chapter IV.

The ERA process starts by forming the pulse response matrices Y(k). Theoretically, pulse inputs are sufficient to excite the system to find the approximate frequency domain transfer function. The impulses must be timed so that they do not all occur at the same time so the individual impulses can overlap and are distinct for each input channel. However, practically a single impulse does not have enough energy to fully excite every state [15]. A method of how this limitation is circumvented is discussed later. The value for Y(0) is not necessary to compute since it is simply the D matrix and consequentially the initial conditions. Each additional pulse response matrix is calculated such that $Y_{i,j}(k)$ is the i^{th} output at sample k resulting from a pulse input on the j^{th} input channel. The dimension of each of the Markov parameter matrices is r x m where r is the number of system inputs and m is the number of system outputs. As the value of k increases, the size of the Hankel matrix composed of the Markov parameters quickly increases. This matrix does not have to be square. As might be expected, the number of Markov parameters used for system identification is larger than the true system model. Ultimately, pulse response matrices can be used to determine the discrete-time model

$$x(k+1) = \hat{A}x(k) + \hat{B}u(k);$$
$$y(k) = \hat{C}x(k) + \hat{D}u(k), \tag{5.2}$$

which is a discretized version of a linearization of (1.25). A basic relationship between the Markov parameters of a system and the input and output relationships can be described by [25]

$$y(k) = \sum_{\tau=0}^{\infty} Y_{\tau} u(k-\tau)\,. \tag{5.3}$$

Therefore the value for the output at sample k can be predicted if the Markov parameters and the previous inputs are known. The first step in the ERA method is finding the Markov parameters of the system. The process of finding the Markov parameters of the system is very important. The method for finding the system realization is well defined by the ERA after these parameters are known. Special care must be taken to ensure that the correct parameters are identified. The system must be excited so that the dynamics of the system can be analyzed. Although, in theory a single impulse function at each of the inputs to the system should provide the necessary test input to find the transfer function between each input and output but in practice a sustained semi-random input is needed [25].

An alternate form of (5.3) can be created not using the actual outputs and inputs but replacing the output term by the cross-correlation between the inputs and the corresponding outputs [25].

$$R_{yu}(i) = \sum_{\tau=0}^{\infty} Y_{\tau} R_{uu}(i-\tau) \tag{5.4}$$

where the length of the data sequence is m,

$$R_{uu}(k) = \frac{1}{m}\sum_{\tau=0}^{m-1} u(\tau)u^{T}(k-\tau) \quad \text{and} \quad R_{yu}(k) = \frac{1}{m}\sum_{\tau=0}^{m-1} y(\tau)u^{T}(k-\tau)\,. \tag{5.5}$$

The basic process for finding the Markov parameters starts using the ratio of the power spectral density of the cross-correlation between the inputs and outputs and the power spectral density of the autocorrelation between the input signals.

These power spectral densities are given by the following

$$P_{yu}(k)=\frac{1}{m}\sum_{\tau=0}^{m-1}R_{yu}(\tau)e^{-j\frac{2\pi k}{m}\tau} \quad \text{and} \quad P_{uu}(k)=\frac{1}{m}\sum_{\tau=0}^{m-1}R_{uu}(\tau)e^{-j\frac{2\pi k}{m}\tau} \tag{5.6}$$

The ratio of the two power spectral densities is the frequency response function and is given by [25]

$$G(z_k)=\frac{P_{yu}(k)}{P_{uu}(k)}. \tag{5.7}$$

Then, the final step is to take the inverse Fourier transform to find the pulse response (Markov parameter) matrices given by the following [25]

$$Y_\tau=\sum_{\tau=0}^{\infty}G(z_k)e^{j\left(\frac{2\pi\tau}{m}\right)k}. \tag{5.8}$$

This system identification method can give good results even in the case where very noisy data is acquired. This ability lies in taking many more Markov parameters than the true system order. The computed Markov parameters that do not agree with the other data can effectively be filtered out of the frequency response function. A Hankel matrix is simply a matrix that is has the i^{th} column identical to the i^{th} row. The Hankel matrix containing the Markov parameters is of the following form:

$$H(k-1)=\begin{bmatrix} Y_k & Y_{k+1} & \cdots & Y_{k+p-1} \\ Y_{k+1} & Y_{k+2} & \cdots & Y_{k+p} \\ \vdots & \vdots & \vdots & \vdots \\ Y_{k+r-1} & Y_{k+r} & \cdots & Y_{k+p+r-2} \end{bmatrix} \tag{5.9}$$

$$H(0)=\begin{bmatrix} Y_1 & Y_2 & \cdots & Y_p \\ Y_2 & Y_3 & \cdots & Y_{p+1} \\ \vdots & \vdots & \vdots & \vdots \\ Y_r & Y_{r+1} & \cdots & Y_{p+r-1} \end{bmatrix} \tag{5.10}$$

The individual Y_k's correspond to the following sequence:

$$Y_0=D,\ Y_1=CB,\ Y_2=CAB,\ \ldots,\ Y_k=CA^{k-1}B \tag{5.11}$$

The Markov parameters are solved for by performing the inverse transform of the frequency response function

$$G(z_k) = \sum_{\tau=0}^{\infty} Y_\tau e^{-j\frac{2\pi k}{l}\tau}; \quad z_k = e^{-j\frac{2\pi k}{l}}. \tag{5.12}$$

The two matrices that are used in the ERA method are H(0) and H(1). Choosing the values for r and p requires some engineering discretion. According to [3] p should be about ten times the number of states that will be identified and r should be about 2 or 3 times as large as p. Concisely, if the desired system model order is 10 and the data is noisy, the number of Markov parameters needed would be about 200 to 300.

The usefulness of the ERA system is closely related with the controllability and observability matrices. The relationship between the Hankel matrix of Markov parameters and the observability and controllability matrices can be seen in

$$H(k-1) = P_r A^{k-1} Q_p \tag{5.13}$$

Then the observability matrix P_r has the following form:

$$P_r = \begin{bmatrix} C \\ CA \\ CA^2 \\ \vdots \\ CA^{r-1} \end{bmatrix}; \tag{5.14}$$

$$Q_p = \begin{bmatrix} B & AB & A^2B & \cdots & A^{p\text{-}1}B \end{bmatrix}. \tag{5.15}$$

If the input matrix B and the output matrix C are defined in the following way,

$$B = \begin{bmatrix} b_1 & b_2 & \cdots & b_r \end{bmatrix} \tag{5.16}$$

and

$$C = \begin{bmatrix} c_1 \\ c_2 \\ \vdots \\ c_m \end{bmatrix} \tag{5.17}$$

where b_i is a column vector that is the control influence vector for the i^{th} input and c_i is a row vector that is the measurement influence vector for the j^{th}

measurement point. The ERA block data can be expressed in the following manner [25]:

$$H(k-1) = \left[Y_{s_i+k+t_j} \right]; \tag{5.18}$$

$$Y_{s_i+k+t_j} = C_j A^{s_i+k-1+t_j} B_i . \tag{5.19}$$

When $i = j = 0$, $Y_k = CA^{k-1}B$. This is a simplified version of (5.9). One advantage of this method of writing the equation is that it represents (5.9) with some rows and columns deleted. Therefore, one major benefit of using the ERA method is the ability to not include some parameters that appear to be distorted or that have very weak values. Consequentially, this reduces the computational requirements by reducing the size of the H matrix but maintaining the data that can be trusted. However, if the data has low noise power, it is possible to use an H matrix that has the number of Markov parameters comparable to the size of the actual state matrix A.

Replacing k-1 with k in equation (5.13) results in the following

$$H(k) = P_r A^k Q_p \tag{5.20}$$

$$P_r = \begin{bmatrix} C \\ C_1 A^{s_1} \\ \vdots \\ C_r A^{s_r} \end{bmatrix} \tag{5.21}$$

$$Q_p = \begin{bmatrix} B & A^{t_1} B_1 & \cdots & A^{t_p} B_p \end{bmatrix} \tag{5.22}$$

A major component of the ERA method is having an approximate pseudo-inverse for the H matrix. This matrix $H^{\dagger}$ must satisfy the following relationship

$$Q_p H^{\dagger} P_r = I_{n\ x\ n} \tag{5.23}$$

The ERA method starts with a singular value decomposition of the H(0) matrix.

$$H(0) = R \Sigma S^T \tag{5.24}$$

The form of Σ shows some information about the remaining singular values after those below a small tolerance are forced to equal exactly 0. Therefore,

$$\Sigma = \begin{bmatrix} \Sigma_n & 0 \\ 0 & 0 \end{bmatrix} \tag{5.25}$$

$$\Sigma_n = \begin{bmatrix} \sigma_1 & 0 & \cdots & 0 \\ 0 & \sigma_2 & 0 & \vdots \\ \vdots & 0 & \ddots & 0 \\ 0 & \cdots & 0 & \sigma_n \end{bmatrix} \tag{5.26}$$

$$\text{with } \sigma_1 \geq \sigma_2 \geq \cdots \geq \sigma_n.$$

Since Σ_n is of size n x n, when R and S^T pre-multiply or post-multiply Σ only the first n columns are nonzero values. Therefore, $H(0)$ takes on a different form.

$$H(0) = R_n \Sigma_n S_n^T \tag{5.27}$$

Then the pseudo-inverse becomes [25]

$$H(0)^\dagger = S_n \Sigma_n^{-1} R_n^T . \tag{5.28}$$

A balanced realization can be created with approximately balanced observability and controllability matrices given by the following relationships [25].

$$\widehat{P_r} = R_n \Sigma_n^{1/2}; \tag{5.29}$$

$$\widehat{Q_p} = \Sigma_n^{1/2} S_n^T . \tag{5.30}$$

Further, looking at the H(1) matrix one can see a relationship between the state matrix A and the H(1) matrix.

$$H(1) = \widehat{P_r} A \widehat{Q_p} = R_n \Sigma_n^{1/2} A \Sigma_n^{1/2} S_n^T \tag{5.31}$$

Then, through simple matrix pre-multiplications and post-multiplications

$$\begin{aligned} \Sigma_n^{-1/2} R_n^T H(1) S_n \Sigma_n^{-1/2} &= \Sigma_n^{-1/2} R_n^T R_n \Sigma_n^{1/2} A \Sigma_n^{1/2} S_n^T S_n \Sigma_n^{-1/2} \\ &= \Sigma_n^{-1/2} I_n \Sigma_n^{1/2} \hat{A} \Sigma_n^{1/2} I_n \Sigma_n^{-1/2} \\ &= I_n \hat{A} I_n \\ \Sigma_n^{-1/2} R_n^T H(1) S_n \Sigma_n^{-1/2} &= \hat{A} \end{aligned} \tag{5.32}$$

If the system has been properly excited in the identification phase, the empirically found triplet $(\hat{A}, \hat{B}, \hat{C})$ is a valid system realization. One important note is that since all the matrix methods used to develop the empirical triplet are linear in

nature. The empirical triplet does not contain any nonlinear terms or time varying elements. However, in [15] a method is described that uses both input to output data and input to state data to better model some of the underlying nonlinear characteristics of the full order system.

First some special matrices need to be defined to extract the $\hat{B}$ and $\hat{C}$ matrices from the empirical data. O_n is a matrix of 0's with dimension n x n. I_n is an identity matrix with dimension n x n. Then, [25]

$$E_p^T = \begin{bmatrix} I_p & O_p & \cdots & O_p \end{bmatrix} \tag{5.33}$$

$$E_r^T = \begin{bmatrix} I_r & O_r & \cdots & O_r \end{bmatrix} \tag{5.34}$$

where r is the number of outputs and p is the number of inputs.

The triplet ($\hat{A}, \hat{B}, \hat{C}$) in the following form gives a minimal system realization

$$\hat{A} = \sum_n^{-\frac{1}{2}} R_n^T H(1) S_n \sum_n^{-\frac{1}{2}}, \tag{5.35}$$

$$\hat{B} = \sum_n^{\frac{1}{2}} S_n^T E_r, \tag{5.36}$$

$$\hat{C} = E_m^T R_n \sum_n^{\frac{1}{2}} \quad . \tag{5.37}$$

The minimal realization is in the sense that all the states are controllable and observable. Further, the system is approximately balanced so that this realization is as controllable as it is observable. It seems that this could be an excellent benefit of using this method, the input and output relationship has been captured from true data. However, since this is an empirical method, the true system dynamics might not be well understood, but should be well predicted for similar inputs to those used in the identification process. A very detailed description of the frequency response function and how to calculate it from empirical data is included in [25].

In some cases the input data for the ERA method might be provided by an experiment on a real system. However, in this thesis a unique approach of using

the linearized Galerkin model in the place of the real system was used to generate the empirical data. The full order system model was created using finite-difference methods. Recall that the control inputs were explicitly placed in the boundary conditions [4] because the control inputs do not show up explicitly in the two-dimensional burger's equation. However, the weak Galerkin model results in a nonlinear state space model that greatly simplifies the relationship between the input and outputs.

As seen in chapter I, the agreement between the finite-difference numerical simulations generated full order model matches the flow of the 40^{th} order Galerkin model very closely. Therefore, the Galerkin model is used as a simplified version of the "system." The 40 order linearized Galerkin model is used to provide outputs from the simulated inputs. This is an example of how a model reduction from a large state size finite element analysis model can be projected on to a relevant subspace and further used to provide an approximated system for empirical data simulations.

The inputs used for the excitation of this Galerkin model are of the following form and are shown in figure 10

$$u_1(t) = -\sin(0.55t^2) \tag{5.38}$$

$$u_2(t) = -\sin(0.60t^2) \tag{5.39}$$

Two model reduction techniques were used with the ERA. These reduction techniques are balanced truncation applied to the empirically identified realization and empirical balanced truncation applied to the linearized Galerkin model.

Figure 11 shows the steps to find the realization ($\hat{A}, \hat{B}, \hat{C}$).

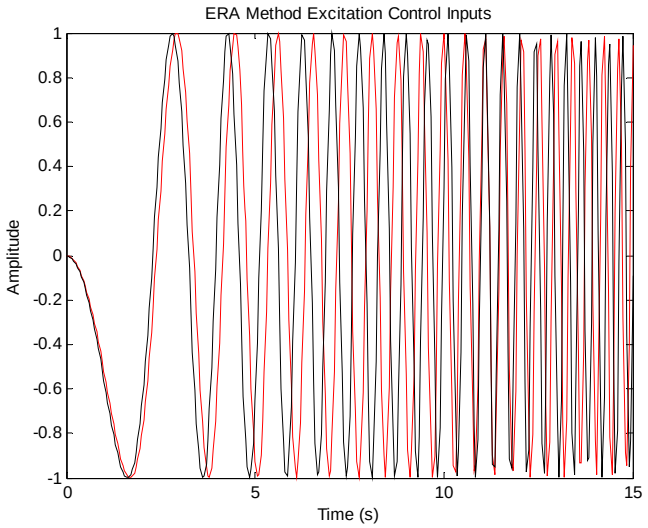


Figure 10. Excitation Inputs for ERA Method

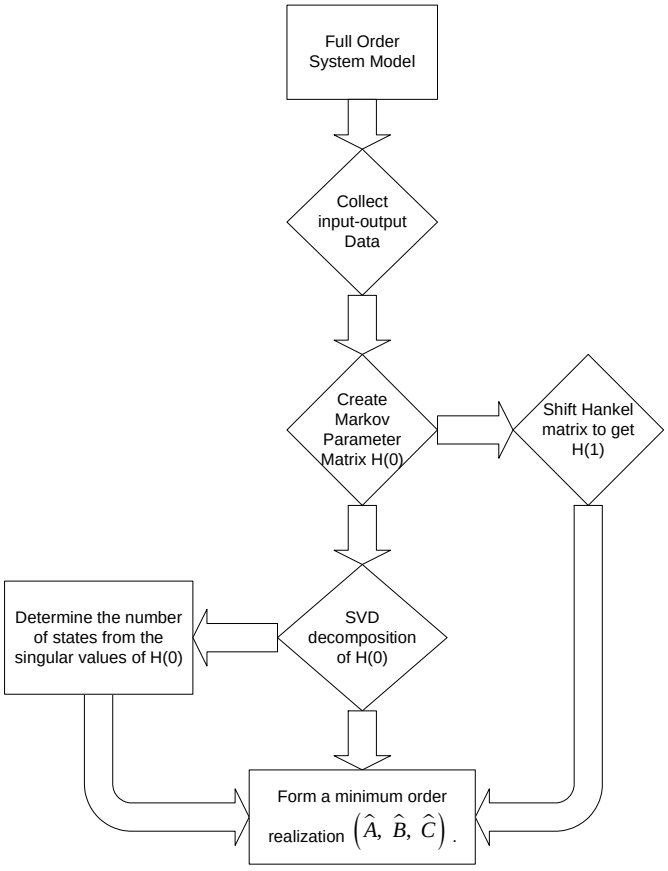


Figure 11. ERA Method Steps Block Diagram

Balanced Truncation

The process for model reduction is very similar to that performed from the POD basis information. However, the method for creating the system realization comes from empirical system information. Therefore, the system that is given by the ERA method is a discrete time system. Care must be taken if one is using this method to perform balanced truncation on a continuous time system by finding the balancing transformation matrix empirically. In this case, if the original system is known, it must be discretized prior to the start of the identification process. The C matrix from the POD model was changed from the identity matrix to a single output matrix given by $C = \begin{bmatrix} 1 & 0 & 1 & 0 & \cdots & 0 & 0 \end{bmatrix}_{1\text{x}40}$. The general balancing method as described with the POD case still holds the same. One major difference is that the ERA system inherently calculates a discrete system realization. Both the input and output samples must be synchronized. This is important to remember for relating the sampling rate to the identified system model. The synchronized input and output sample data is absolutely necessary so that the pulse response of the system can be retained.

All the steps for the balanced truncation are described in chapter IV under the balanced truncation section. One must only substitute the empirically found triplet $\left(\hat{A}, \hat{B}, \hat{C}\right)$ for the values for $\left(A, B, C\right)$ in the development. However if the balancing is desired for the discrete system, then there is one very important difference between the temporal equation case of balanced truncation and the ERA case. The primary difference is that the discrete time Lyapunov equations must be solved for the controllability and observability Gramians instead of the continuous time Lyapunov equations as in (4.7) and (4.8). The same conditions of stability are placed on the discrete time case as the continuous time case. These equations can be written as

$$AW_c A^* - W_c + BB^* = 0 \tag{5.40}$$

$$A^* W_o A - W_o + C^* C = 0\,. \tag{5.41}$$

Then, the procedure can be followed as in equations ((4.15) to (4.28)). This new balanced and truncated realization can then be used directly for control design or can be converted to a continuous time system for simulation or comparison with a true continuous system. There will be some error in the approximated system when compared with the true system. However, this error will be small if the signals used for system identification with the ERA method are similar to the signals that will actually be used in system operation.

Empirical Balancing Truncation

Very closely related to the ERA system identification method is a method of finding directly the empirical controllability and observability Gramians from experimental or simulated data. This method has a different goal from the ERA method. The rational and details of this method are described as empirical balancing truncation in ([13] and [14]). Unlike the general ERA method, the realization from the empirically approximated system is not the primary product. This method does not directly find the realization from the empirical data, but is targeted specifically in solving the empirically found observability and controllability Gramians. The ultimate goal is actually to find the balancing transformation matrix T that will approximately balance the empirical Gramians. This T matrix can then be applied back to the original system model to produce an approximately balanced realization.

Unlike the general ERA method, the number of states and consequentially the empirical state matrix A's size will have to be the same as the full order system's A matrix. Of course since a balancing transformation matrix is needed, the matrices must be appropriately sized so that the matrix multiplication can occur. A practical use for this process is to find an approximate balanced truncation for a nonlinear system model from a balanced empirically found linear system

model. A few additional steps are needed to find an appropriate balancing transformation from a system that is highly nonlinear [15].

All the necessary information to calculate the empirical Gramians is actually included in the ERA method. The ERA method inherently calculates the empirical Gramians. Recall that the Markov parameters of the system are of the following form.

$$Y(0) = D,\ Y(1) = CB,\ Y(2) = CAB,\ \cdots,\ Y\left(k\right) = CA^{k-1}B\,. \tag{5.42}$$

The Hankel matrix containing the Markov Parameters is actually a result of the multiplication of a multiple step observability matrix and a multiple step controllability matrix.

Define the l-step controllability matrix and the q-step observability matrix as

$$Q_{p_l} = \begin{bmatrix} B & AB & \cdots & A^{l-1}B \end{bmatrix}, \tag{5.43}$$

$$P_{r_q} = \begin{bmatrix} C & CA & \cdots & CA^{q-1} \end{bmatrix}^T. \tag{5.44}$$

Then the product of the l-step controllability and the q-step observability matrices gives a Hankel matrix containing the approximated Markov parameters of the system in the following way.

$$P_{r_q}Q_{q_l} = H(0) = \begin{bmatrix} CB & CAB & \cdots & CA^{q-1}B \\ CAB & CA^2B & \cdots & CA^qB \\ \vdots & \vdots & \ddots & \vdots \\ CA^{l-1}B & CA^lB & \cdots & CA^{l+q-2}B \end{bmatrix} \tag{5.45}$$

This product is the $H(0)$ matrix used in the ERA method. These Markov parameter values are found empirically so this matrix will not be a perfect Hankel matrix with the required symmetry. This realization shows how the general ERA method is related to this process since this matrix is created in the ERA method. Figure 12 shows the basic idea of this method to use an empirically found balancing transformation matrix to balance the original system.

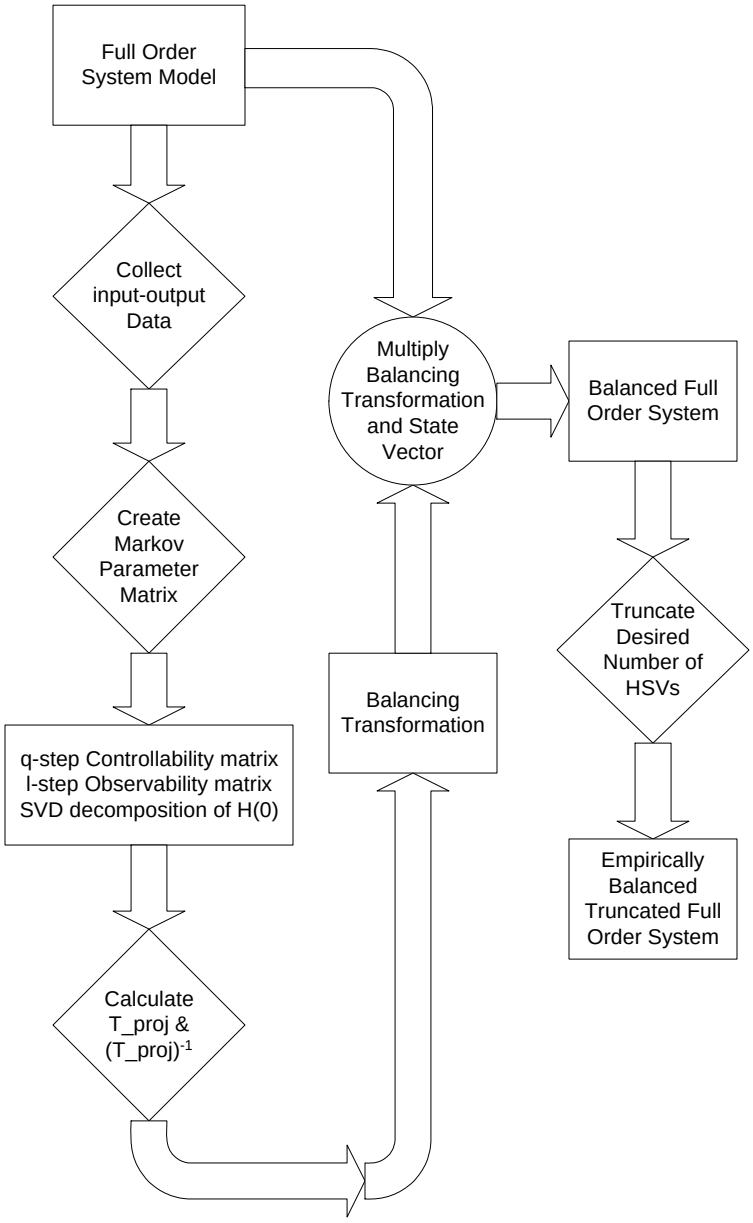


Figure 12. The Empirical Balanced Truncation Method

Equation (5.45) makes an important connection between the Markov parameters and the product of the observability and controllability matrices of the system.

At this point, the empirical Gramians can be found from the following relationships [27]

$$W_{c_l} = Q_{p_l}^T Q_{p_l} \tag{5.46}$$

$$W_{o_q} = P_{r_q} P_{r_q}^T \tag{5.47}$$

As the number of steps q and l approach infinity, these empirical Gramians approach the true Gramians. Then, a transformation matrix, T must be found such that the Gramians are balanced and equal as in

$$\widehat{W_{c_l}} = T^{-1} W_{c_l} \left(T^{-1}\right)^T = \Sigma_1 \tag{5.48}$$

$$\widehat{W_{o_q}} = T^T W_{o_q} T^{-1} = \Sigma_1 . \tag{5.49}$$

Now, the balanced empirical Gramians have been identified and can be used to perform the standard balanced truncation model reduction technique.

The approximate value for the q-step controllability matrix can be found in the following way from the empirical data [27].

$$\widehat{Q}_{p_l} = \Sigma^{-1/2} R^T H(0) \tag{5.50}$$

where $\Sigma,\ R,$ and $H(0)$ are defined as in equation (5.24).

The balancing transformation matrix is given by

$$T_proj = Q_{p_l} V_n \Sigma_n^{-1/2} \tag{5.51}$$

and since the Gramians are approximately balanced

$$(T_proj)^{-1} \simeq \Sigma_n^{1/2} (Q_{p_l} V_n)^{\dagger} . \tag{5.52}$$

These projection matrices can be used to balance the full order system. Then, truncation of the HSVs that have small values results in an approximate balanced truncation [15].

The realization for the reduced balanced realization is given by the solution of the following,

$$A_r = (T_proj)^{-1}\widetilde{A}(T_proj) \tag{5.53}$$

$$B_r = (T_proj)^{-1}\widetilde{B} \tag{5.54}$$

$$C_r = CT_proj \tag{5.55}$$

The reduced balanced truncation realization of the state space model described by equations (1.30) and (1.31) is then obtained.

CHAPTER VI
RESULTS AND OBSERVATIONS

Now that the mathematics and some specific methods have been discussed, the results of some specific cases are discussed. The results of using system model reduction methods on the original system model given in the form of a Galerkin projection on a POD basis and some observations are presented in this chapter. Further, the frequency domain system identification techniques are analyzed for their effectiveness. Most importantly the results from using the Galerkin model as the test system is used to show proof of concept of the effectiveness of the ERA method to the two-dimensional Burger's equation. Further, the empirical Gramians can be found and used to empirically balance and then truncate the original system with very good results.

POD Basis Truncations

The Galerkin model gives a reasonably good approximation to the full order model. Fortunately the weak solution provided by the Galerkin projection, can further be reduced to provide even smaller system models. This is an important observation because the POD basis in this process could have originally been chosen to be 50 or 100 modes. The scree plot test shows that the 'scree' definitely begins somewhere after 25 modes and perhaps as early as after 15 modes. Because of the ability to reduce the order of the POD basis to less than 40 "true" modes, the reduced models (from the larger 50 or 100 original POD modes) likely would be reducible to the same degree as the temporal model given by 40 modes.

The balanced truncation was selected to maintain 14 states. The match for the first 10 outputs is very close to the 40 order nonlinear model even though only a

small number of the HSVs have been retained. The last HSV retained only has a value of slightly less than 1e-3.

In the case of the Hankel Optimal Norm Approximation Model Reduction it was determined that only 8 states need to be retained. However, the Hankel Optimal Norm Approximation method matches the full order outputs much better than the standard balanced truncation even though the latter has retained 6 additional states.

Figure 13 shows that the matching of the first 7 Hankel singular values match very well for the 40th order temporal model and the system realization that is truncated to 8 states with the Hankel optimal norm approximation method. The HSVs from the balanced truncation case are not shown, as they are a subset of the full order case's Hankel singular values.

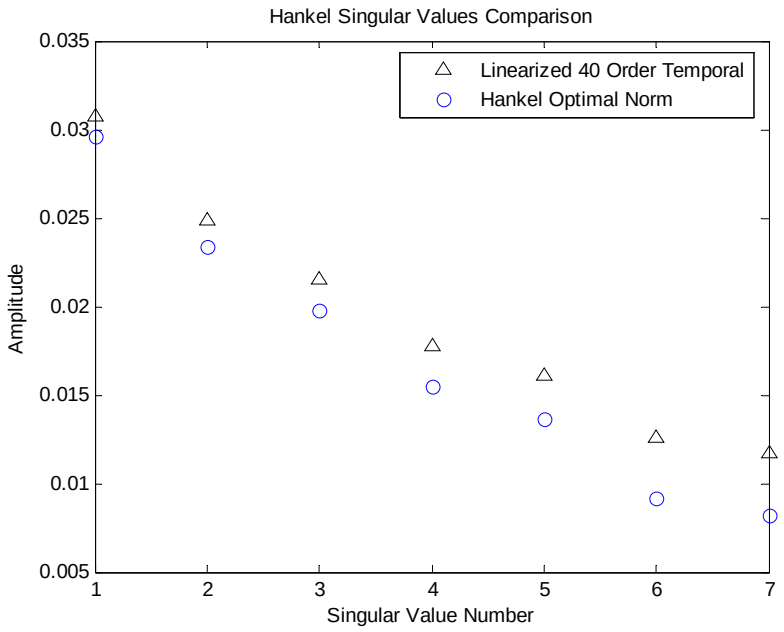


Figure 13. Comparison of Full Order HSVs and Hankel Optimal Norm HSVs

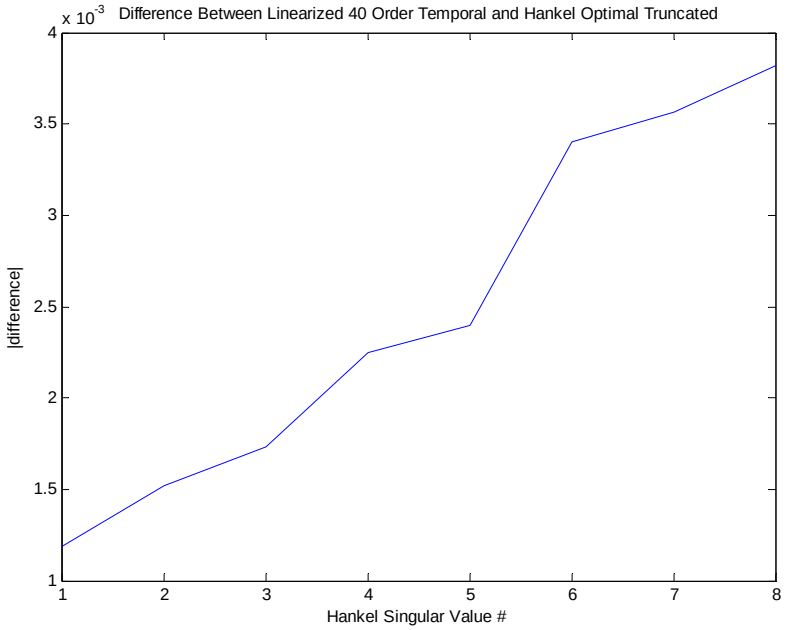
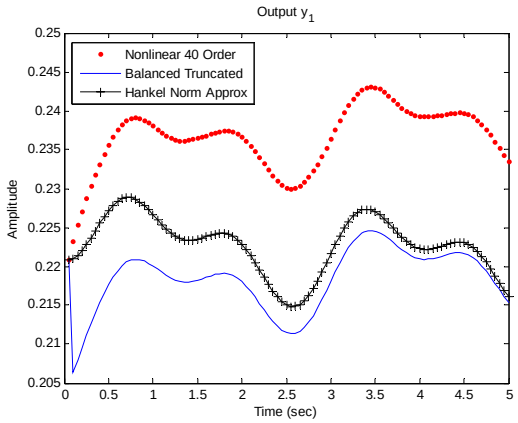


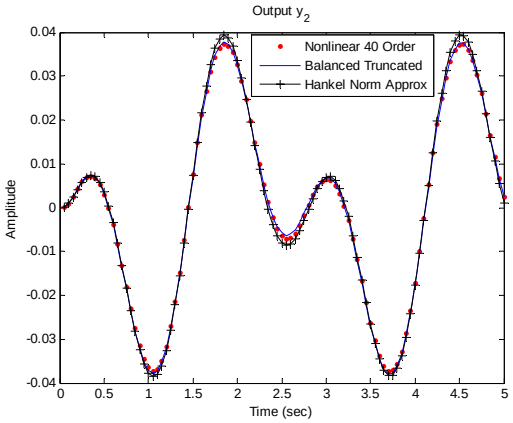
Figure 14. Balanced Truncated and Hankel Approximation Difference

Figure 14 shows the difference between the HSVs of the linearized 40-order Galerkin model and Hankel optimal norm approximation model. The difference increases in magnitude as the order of the HSV increases. Since the first few HSVs are the most important this is a very good finding. Ultimately we are concerned that the input-output behavior of the two models is very similar. However, we conclude that the HSVs for the Hankel optimal norm approximated model gives approximately the same importance to each of the input-output pairs as does the linearized 40-order Galerkin model.

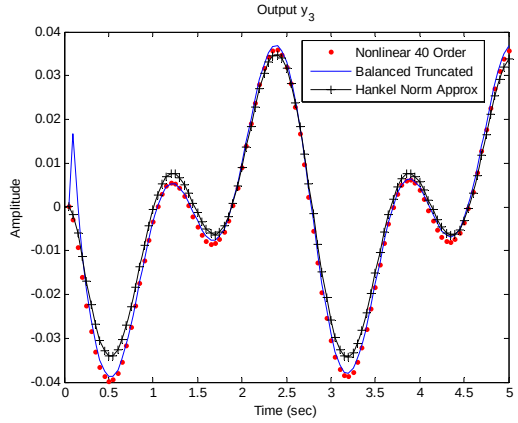
Figure 15 shows the comparison of several outputs produced by three different mathematical models. The dotted line is the output from the nonlinear 40^{th} order temporal model, the solid line is the output from the balanced truncated model, and the crossed line is the output from the Hankel norm approximation reduced order model. Both the balanced truncation and Hankel optimal norm approximation techniques began with the 40^{th} order temporal model linearized about the initial conditions.



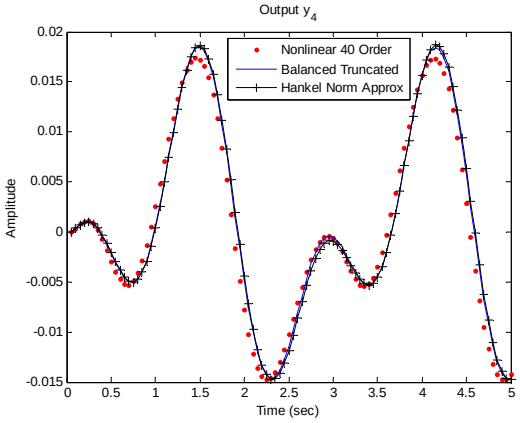
(a) First output: $y_1(t)$



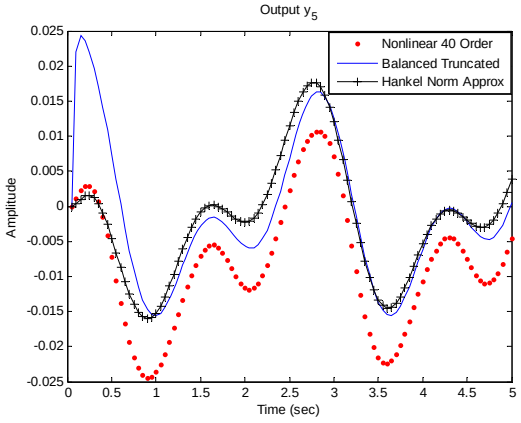
(b) Second output: $y_2(t)$



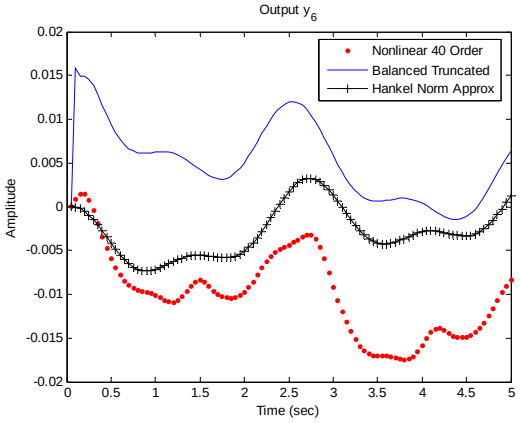
(c) Third output: $y_3(t)$



(d) Fourth output: $y_4(t)$



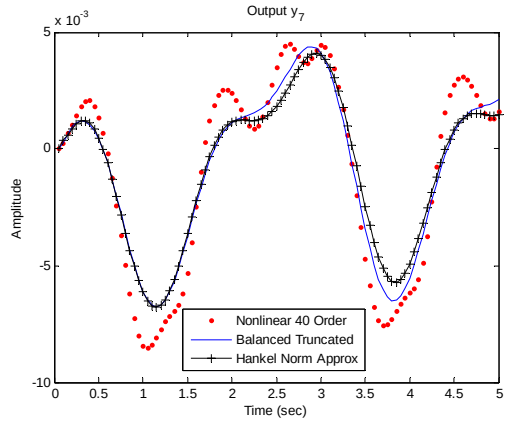
(e) Fifth output: $y_5(t)$



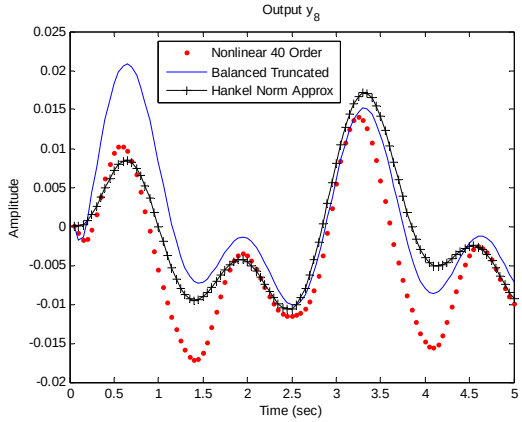
(f) Sixth output: $y_6(t)$

Figure 15. Output Comparison of Reduced Models to Nonlinear 40 Order Model

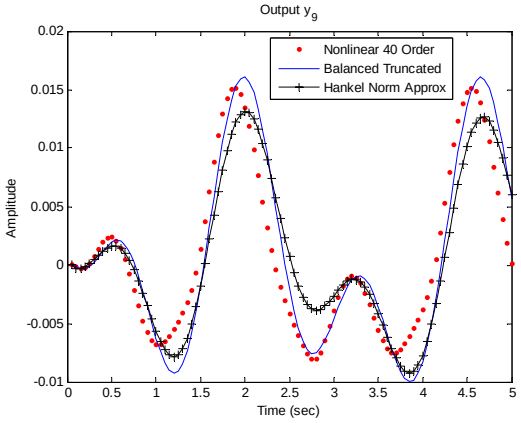
Figure 15. Continued



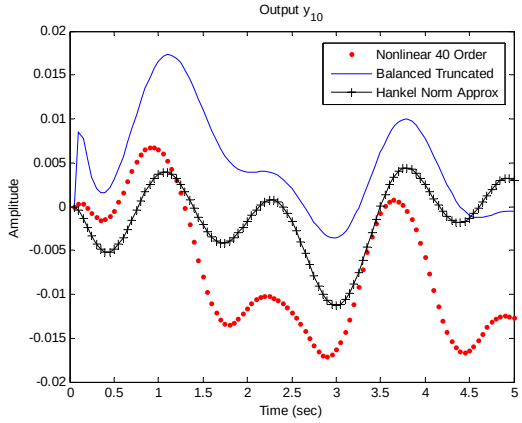
(g) Seventh output: $y_7(t)$



(h) Eighth output: $y_8(t)$



(i) Ninth output: $y_9(t)$



(j) Tenth output: $y_{10}(t)$

The Hankel optimal norm approximation system tracks the original output very well (as seen in figure 15). The original (dotted) plot is used as a reference to compare the relative effectiveness of the two model reduction techniques. With the exception of the 5^{th} and 9^{th} outputs, the Hankel norm approximation reduced model gives better or comparable tracking to the nonlinear reference than the balanced truncated model. In the case of every output, both the Hankel norm approximation and balanced truncated models give very close results to the reference nonlinear model and match most of the system dynamics.

Table 1 shows the theoretical upper bounds on the H-infinity norm of the difference between the linearized 40 state Galerkin system model and the proposed reduced system. This of course does not give a tight bound on the error. But, it does give some idea about the worst-case situations. An example of how this information might be useful is to compare the case with 12 states remaining on the Hankel optimal norm and 14 states remaining with the balanced truncation method. The Hankel norm approximated system has a lower upper bound even though it retains 2 fewer states. The importance here is that these are states that have fairly large Hankel singular values in comparison to the 20 smallest HSVs. However, from the results seen, the Hankel optimal norm approximation gave a better approximation for almost all of the outputs than the balanced truncation retaining several additional states.

Although the individual outputs for the reduced models match well with the nonlinear temporal model created from the Galerkin projection, the flows of the systems should be compared. The flow is what must be controlled. Controlling a single output would not control the entire flow. The flow is a combination of the outputs as they apply to the flow of the fluid through the problem geometry. Here the output matrix C was a 40 x 40 identity matrix. The flows for the nonlinear model and the Hankel norm approximation and the balanced truncation are shown together in figure 16.

Table 1. Balanced Truncation and Hankel Model Reduction Error Bounds

States Remaining	*Balanced Truncation Error Upper Bound*	*Hankel Optimal Norm Error Upper Bound*
40	0	0
30	1.75e-4	8.74e-5
20	4.98e-3	2.49e-3
14	2.59e-2	1.30e-2
12	4.23e-2	2.12e-2
10	6.67e-2	3.34e-2
8	1.02e-1	5.08e-2

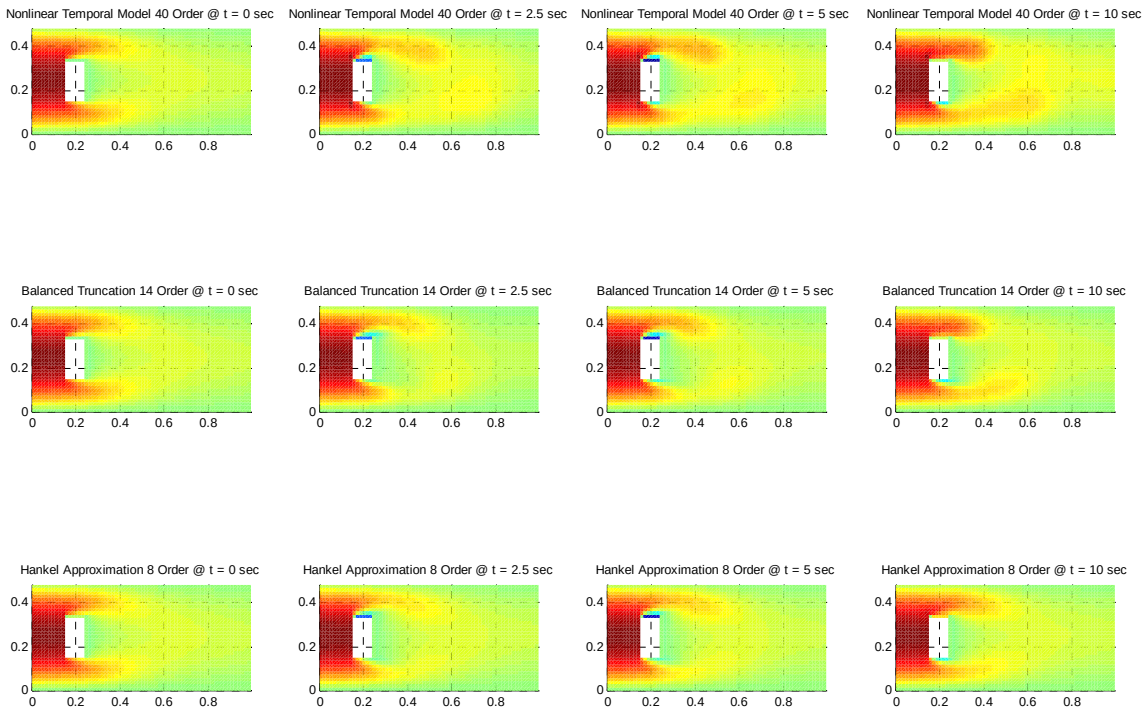


Figure 16. Temporal Model Flow Comparisons

ERA Method Applied to the Linearized Temporal Model

The ERA method will now be applied to the Galerkin projected model. The linearized Galerkin model is considered to be the full order, true system model for identification purposes. In this case the linearized temporal model was excited by white noise to create the Hankel matrix that is needed to perform the ERA system identification procedure.

Since we first wanted to verify that the ERA method was capable of detecting the linearized system model's Markov parameters, the linearized temporal model was used as the system to be identified. This choice is justified since the balanced truncation model reduction technique will be used on the linearized model. Several advantages come from this choice of a system for identification. First, since the Galerkin projected model is known, the effectiveness of the system identification can be evaluated. Second, it is possible to compare the balanced truncation model reduction directly from the Galerkin projected model with the balanced truncation model based upon the ERA method identified empirical model.

The ERA Method's predicted system realization of a Multiple input single output (MISO) system based upon the linearized temporal model from the Galerkin projection of the two-dimensional Burgers equation on the POD basis can be used to show the effectiveness of the frequency domain system identification parameters. Specifically, this effectiveness is shown by a comparison with the linearized temporal model based upon the weak solution to the two dimensional Burger's equation. Further, balanced truncation is performed on the approximated system in figure 17 that shows that additional model reduction can effectively be performed on the ERA created model. The C matrix that was used is $\begin{bmatrix}1 & 0 & 1 & 0 & \cdots & 0 & 0\end{bmatrix}$ a 1x40 row vector. Using this output matrix, C, the output seen in figure 18 was produced.

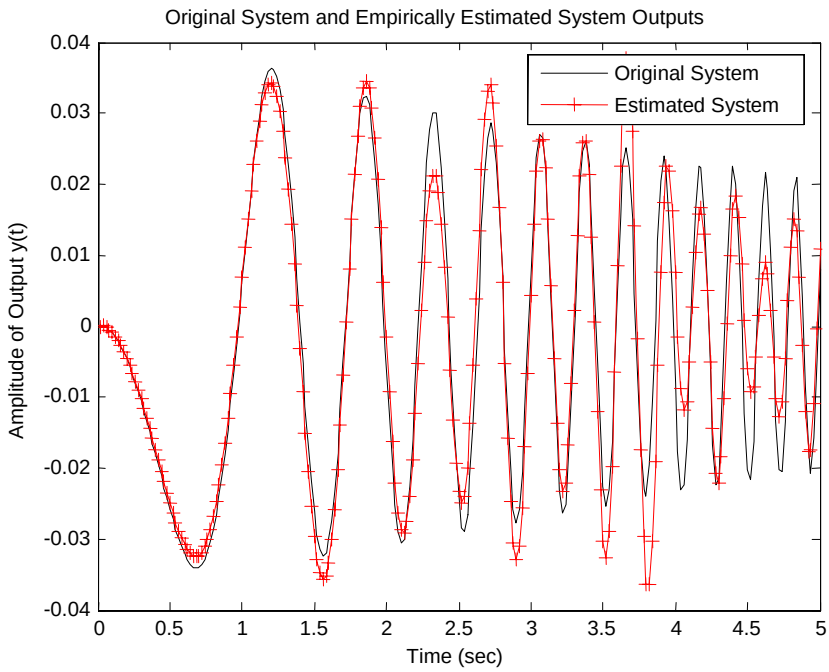


Figure 17. ERA Estimated System Output Approximation from Galerkin Model

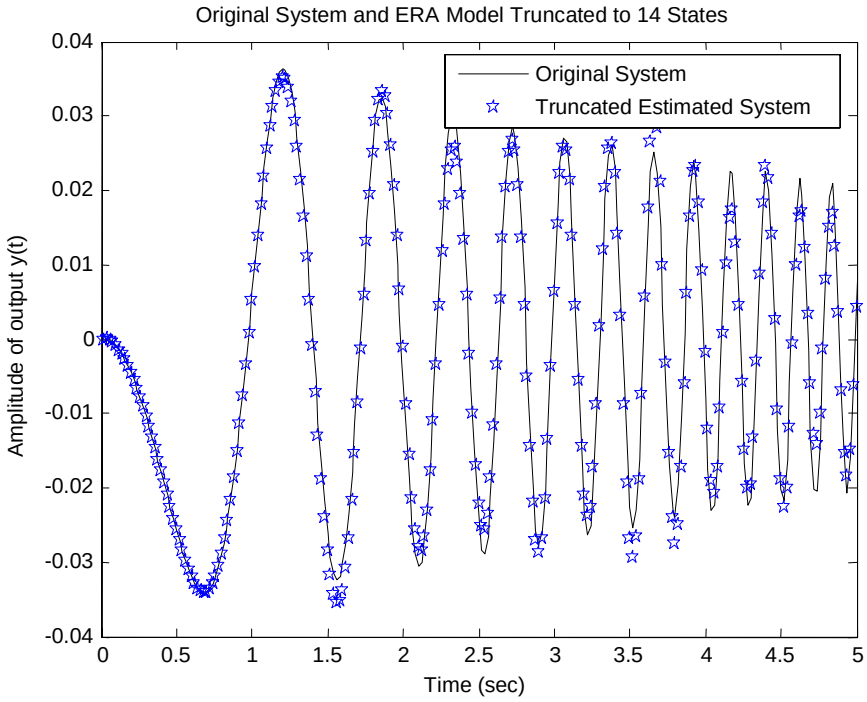


Figure 18. ERA Estimated System Balanced Truncation

Table 2. System Identification ERA Parameters Used

ERA Method Parameters	*Value Used*
Horizontal entries in $H(0)$	60
Vertical entries in $H(0)$	60
Sample time (dt)	0.02 seconds
States desired	40
Input-output samples	1251

Table 2 shows very important information about the ERA method. The first step in the ERA method is to choose how many input-output samples are desired. Further, the sample time (given here as 0.02 seconds) determines how often samples of the input-output data are recorded. The value for the horizontal entries in the $H(0)$ matrix does not describe the number of columns of in the $H(0)$ matrix but the number of columns of Markov parameters included in this Hankel matrix. In the same way, the value of vertical entries in the $H(0)$ matrix gives the number of rows of Markov parameters included in the Hankel matrix. In this case each Markov parameter has dimension 2 x 40 (inputs by output). Therefore the dimensions of $H(0)$ is (60 x 2) x (60 x40) = 120 x 2400.

The entry for ‘states desired’ refers to the number of states that will be identified by the ERA method. In this case, the actual number of states is known to be 40. However in general, the number of states to be identified is a design choice. In the ERA method the value for ‘states desired’, must be less than the minimum of the values for horizontal entries in $H(0)$ and vertical entries in $H(0)$.

Empirical Balanced Truncation

The results from the previous section show that the ERA method was successful in creating an approximate system realization from empirical data. Now, the

frequency domain methods were applied to finding the empirical Gramians and to consequentially find the balancing transformation matrix. The transformation matrix was then found. Then balancing was preformed as described in equations (5.53) to (5.55) with the empirically found balancing transformation applied to the linearized Galerkin model. This empirically balanced truncated model was reduced to maintain 14 states like the balanced truncated model that resulted from the linearized Galerkin model. Therefore, an equitable comparison between the two model reduction techniques can be made. If the balancing transformation matrix is found using the empirical Gramians to match exactly with the true balancing transformation, the empirical balanced truncated model would exactly match the balanced truncated model formed from the linearized temporal Galerkin model.

To ensure that there is good agreement between the two model reduction techniques, the linearized Galerkin model's HSVs are compared with the HSVs of the system that was balanced with the empirical balancing technique. Good agreement will show that the system realization has been balanced. Figure 19 shows very close agreement between the HSVs. Therefore, we can be sure that the empirically found balancing transformation matches closely with the balancing transformation found using the standard method in chapter IV. The values for the HSVs would be exactly equal if the empirically found Gramians had been exactly equal to those of the true linearized 40-order Galerkin model.

Figure 20 shows very close agreement for the first five outputs of the Galerkin balanced truncated model and the empirically balanced truncated model. The close matching again shows that the empirically found balancing transformation is very similar to the balancing transformation found in the standard manner. The goal of producing the same input-output behavior has been achieved. This empirical method also allows the use of balanced truncation while retaining good agreement with the 40-order Galerkin model's input-output behavior.

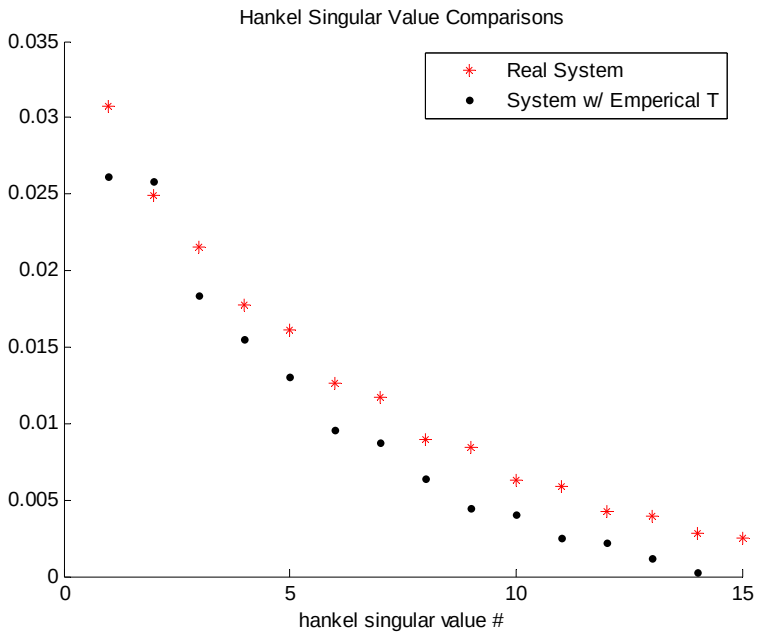


Figure 19. Linearized Galerkin and Empirically Balanced System's HSVs

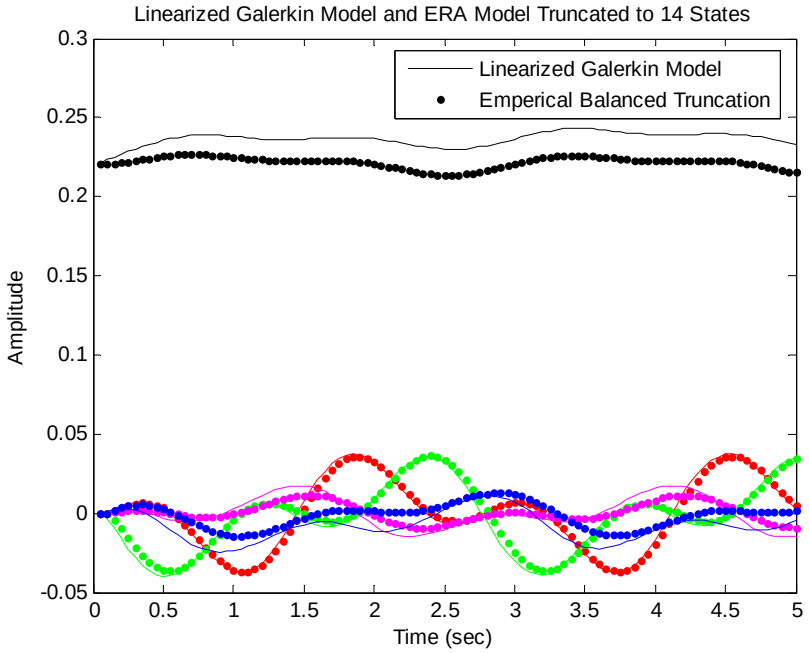


Figure 20. First 5 Outputs for Temporal and Empirically Balanced Truncated

Table 3. Emperical Gramain ERA Parameters Used

ERA Method Parameters	*Value Used*
Horizontal entries in $H(0)$	120
Vertical entries in $H(0)$	120
Sample time (dt)	0.05 seconds
States desired	40
Input output samples	120

Table 3 includes the parameters used in the ERA method for the system identification. Table 3 varies from Table 2 in a few ways. One major difference is that this ERA method instance uses a 50 ms sample time versus the 20 ms sample time. Further all of the 120 input-output samples are used in the ERA method. The total size of the $H(0)$ then is (120 x 2) x (120 x 40) = 240 x 4800. Better approximations might be possible with a larger Hankel matrix. With 512 input-output pairs, the Hankel matrix would have been of size 1024 x 20480.

Figure 21 shows that the balanced truncation from standard methods matches very well with the empirical balanced truncation method. In both cases the balanced truncation was truncated to 14 states. Further, it was found that the Hankel optimal norm approximation more closely followed the input-output behavior of the full order system than the balanced truncated model. The Hankel norm approximation only retained 8 states. There is some small variation between the empirically balanced truncation output y_5 (corresponding to x_5 since the identity matrix is used for C) and the temporal model created by a Galerkin projection onto the POD basis. The two balanced truncation methods match very closely. Since the outputs match well for both of the methods, we conclude that the empirical balanced truncation method is a valid and useful model reduction technique.

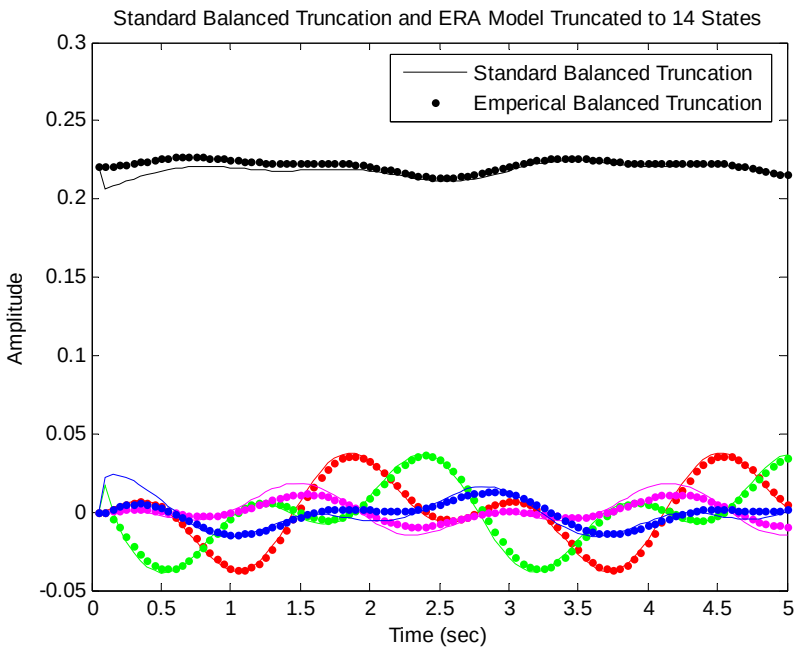


Figure 21. Validation of Empirical Balanced Truncation

As with the comparison of the two model reduction techniques with the original nonlinear temporal model, the comparison of the flow is the true test for similarity. The flow, or combination of all the outputs, is the object that must be controlled. Here the output matrix C is also chosen to be a 40 x 40 identity matrix. Figure 22 shows output flows from two different reduced order models. The first model reduction was preformed by the empirical balancing truncation method. The second model reduction was performed by the standard balancing truncation method. Output flows from both of the models match very closely. This result shows that the empirical balanced truncation method can be used with the linearized Galerkin model to produce similar results to the standard balanced truncation method. Therefore, the empirical balancing truncation method can be used to perform model reduction without knowing the true controllability or observability Gramians.

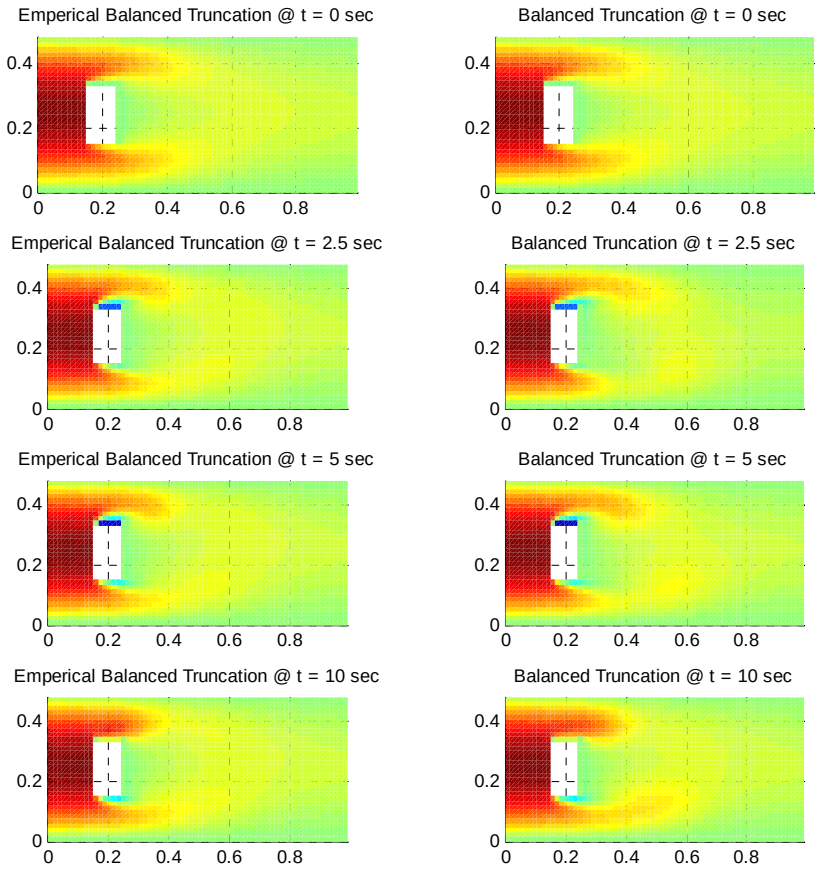


Figure 22. Flow Comparison: Standard Versus Empirical Balanced Truncation

CHAPTER VII
CONTROL DESIGN FOR PDE'S

In the context of solving very complex NPDEs control design the choice of control design methods is very important. In this thesis the 'Reduce then Design' method is used for control design. After a model reduction technique has been used, the control design can be fully implemented. Although the POD method requires some assumed control in order to fully form the initial model, more complete control design can be implemented after model reduction. Of course the very act of calculating the Galerkin state-space temporal model of the system has reduced the system states greatly. Again the debate mentioned in chapter II returns. One must decide whether to do design with the full order model and then reduce the controller or to reduce the plant first and then do control design. If computer calculation speed and memory space were both infinite, control design before reduction would not cause any problems. Further, there would be no concern in implementing the control in real time. The frequencies that are important for control must be considered. In the problem we consider in this thesis, low frequencies are much more important than high frequencies. Here we only consider control for the purpose of completeness but additional comments on control are included in chapter VIII. Since computation speed is not infinite nor is memory size infinite, in some cases the control design simply cannot reasonably be done with a full order nonlinear system. In the case of the 2-dimensional burger's equation, or ultimately in the multi-dimensional Navier-Stokes equation, computational constraints usually dictate a 'Reduce-then-Design' approach.

LQR Control Formulation

One possible method for control design for PDE based problem is the linear quadratic regulator (LQR) control method ([4], [5], [27]). The LQR control method provides an optimal controller in the H^2 space. The control formulation begins

with the linearized state-space equation (1.30) and (1.31). The linearized model for tracking conditions has the form

$$\begin{bmatrix} \dot{\alpha} \\ \alpha_{ref} \end{bmatrix} = \begin{bmatrix} A & 0 \\ 0 & 0 \end{bmatrix} \begin{bmatrix} \alpha \\ \alpha_{ref} \end{bmatrix} + \begin{bmatrix} B \\ 0 \end{bmatrix} u \tag{7.1}$$

$$= \overline{A}X + \overline{B}u, \tag{7.2}$$

where $\overline{A}$ and $\overline{B}$ are augmented to hold the reference state values

$$\overline{A} = \begin{bmatrix} A & 0 \\ 0 & 0 \end{bmatrix} \quad \text{and} \quad \overline{B} = \begin{bmatrix} B \\ 0 \end{bmatrix} \tag{7.3}$$

and

$$\mathrm{X}(t) = \begin{bmatrix} \alpha(t) \\ \alpha_{ref} \end{bmatrix} \quad ; \quad \mathrm{X}(0) = \begin{bmatrix} \alpha_0 \\ \alpha_{ref} \end{bmatrix}. \tag{7.4}$$

This control method is based on minimizing the γ shifted cost function

$$J(\alpha_0, u) = \int_0^\infty \left\{ (\alpha - \alpha_{ref})^T Q(\alpha - \alpha_{ref}) + u^T R u \right\} e^{2\gamma t} dt \tag{7.5}$$

for all control values.

$$u_{opt} = -KX \tag{7.6}$$

$$= -\begin{bmatrix} K_1 & K_2 \end{bmatrix} X \tag{7.7}$$

$$= -\begin{bmatrix} R^{-1}B^T\Pi_{11} & R^{-1}B^T\Pi_{12} \end{bmatrix} X, \tag{7.8}$$

The value for Π_{11} is the solution to the following algebraic Riccati equation

$$(A + \gamma I)^T \Pi_{11} + \Pi_{11}(A + \gamma I) - \Pi_{11} B R^{-1} B^T \Pi_{11} + Q = 0 \tag{7.9}$$

and the value for Π_{12} is the solution to the equation

$$\left[(A + \gamma I)^T - \Pi_{11} B R^{-1} B^T \right] \Pi_{12} = Q. \tag{7.10}$$

This control placed into the linearized model results in the new closed loop system

$$\dot{\mathrm{X}} = (\overline{A} - \overline{B}K)\mathrm{X}, \tag{7.11}$$

$$\mathrm{X}(0) = \mathrm{X}_0. \tag{7.12}$$

LQR Control Results

The LQR control method was applied to both the balanced truncated Galerkin model and the Hankel norm approximation reduced order system. Figure 23 shows the flow that is used for the reference in this control problem. Further, the initial condition projected onto the POD basis is show. The initial flow does not look very similar to the desired reference control. Therefore, the initial conditions cannot possibly match the reference flow. The control objective is trying to limit the 'hot' parts of the flow (depicted by red and orange) from traveling in the y-direction (refer back to figure 1 for the axis orientation designation). The control's effectiveness can be evaluated by its ability to limit the 'hot' portion of the flow's presence beyond the obstacle in the problem space. The first mode is the primary mode of importance. However, the control inputs are used to control the other modes as well.

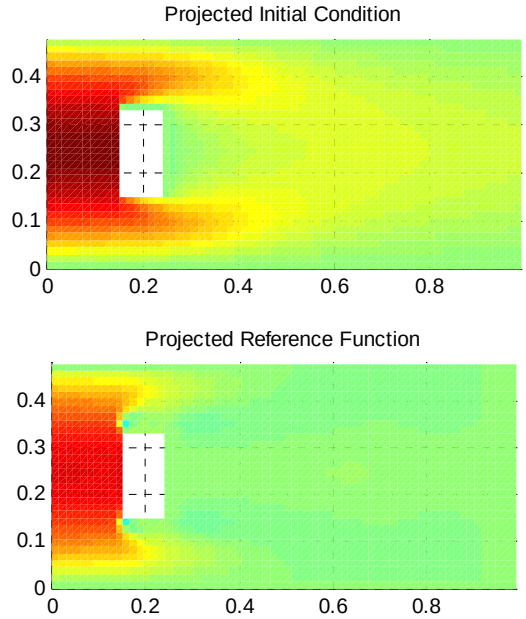


Figure 23. Desired Reference Flow for Control and Initial Flow Condition

The controlled output for the balanced truncated model is shown in figure 24. The flows for both the full order model from the snapshots and the reduced order (by balanced truncation) controlled model is shown at four distinct times. The controlled balanced truncated model's flow matches the desired reference flow in each of the time plots very well, while the full order snapshot method shows the flow without control. The controlled Hankel optimal model approximation model's flow is also compared in figure 25 with the full order snapshot model with similarly beneficial results.

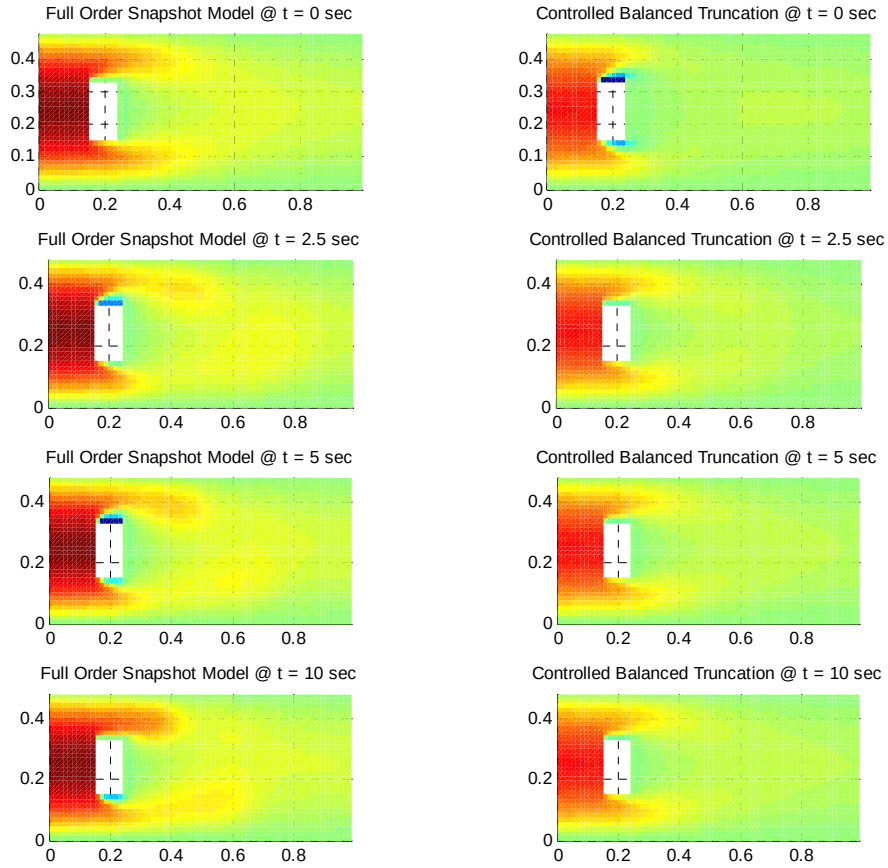


Figure 24. Control Applied to the Balanced Truncation Reduced Model

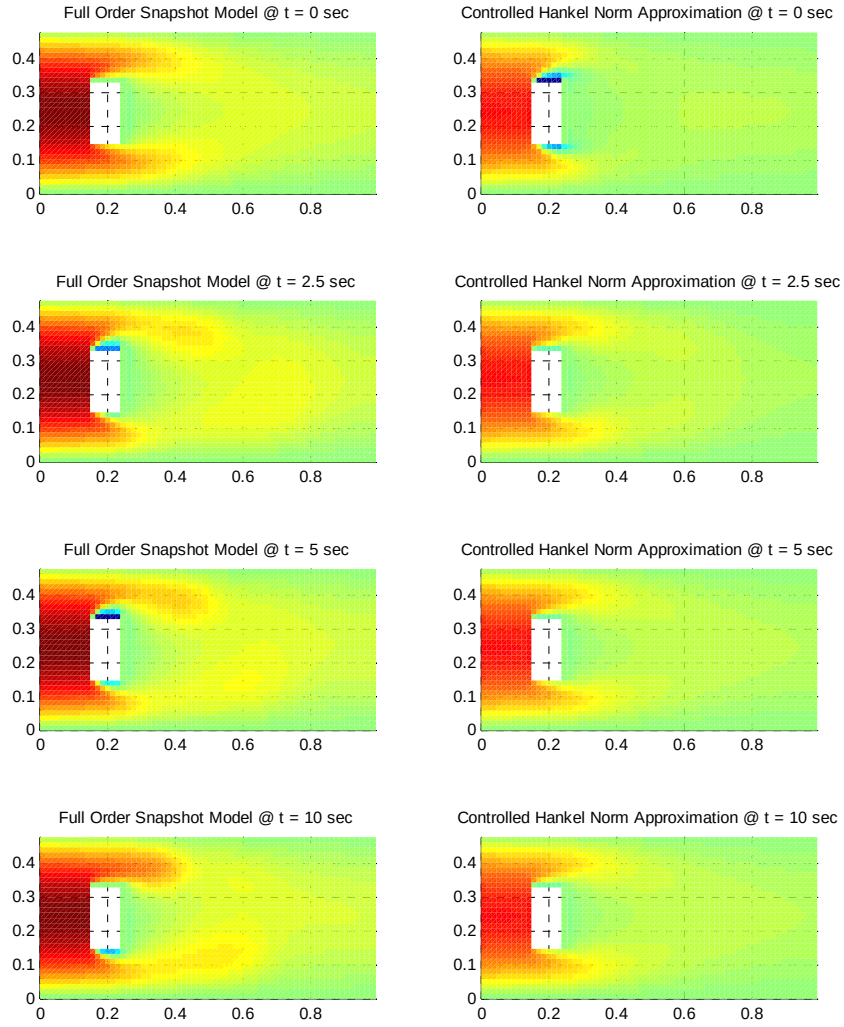


Figure 25. Control Applied to the Hankel Optimal Norm Approximation Reduced Model

The controlled Hankel optimal norm approximated reduced model's flow matches the reference flow in figure 23 very closely.

CHAPTER VIII
CONCLUSION

Methodology

The need for model reduction is often essential to make the system model solution tractable. Model reduction in itself attempts to reduce the size of the realization matrices while preserving the most important information about a system. The first step in model reduction is to achieve a reliable “full-order” system model. When using CFD based approaches, the order of the system is selected by the designer without knowledge of how many of the states will contain necessary system dynamics. This problem remains with other approaches as well. The ERA method does not have any way to know *a priori* the number of states that will be needed. Fortunately with this method, one can evaluate a small Hankel matrix of the system Markov parameters to see if the relative difference between the Hankel singular values is becoming very large. The Hankel matrix, equation (5.10) can then be progressively increased in size. For systems with very large initial model sizes, it is very likely that a ‘reduce-then-design’ approach must be used to facilitate fast simulation and control design. In this thesis, the choice to use only 40 POD basis vectors for the “full order temporal model” was made since these 40 modes were sufficient to capture more than 99.9% of the total energy. Further, the 40^{th} order Galerkin model matched the full order finite-difference solved flow solution very closely.

The ERA method presents its own challenges. The method works best when the states are all fully observable. The ERA method finds an effective minimal realization *de facto* due to the fact that weakly observable and controllable states are not represented strongly in the approximated realization. However, to get a very accurate model for a highly nonlinear model, the input to state information is also needed to find the controllability matrix that is needed to compute the empirical Gramians. When the ERA method was attempted with a 40 x 40

identity output matrix, the computer system often would run out of memory while trying to build the Hankel matrix. In order to find a good quality empirical model a fairly large Hankel matrix must be found. One potential problem with the ERA method is the memory requirements needed to develop a high quality empirical model if the number of inputs and outputs to the system is high. Ultimately, the system was reduced to a 20 state system so that there were no memory problems. Simulations were run to insure that the Galerkin model containing only 20 states gave very similar outputs as the 40-state Galerkin temporal model that was also checked with the full order flow solution from the finite-difference numerical solution.

Choosing Modes

The number of modes to include in these model reduction methods is an area for engineering design. Some guidelines may be summarized as follows: The Hankel singular values give a quantitative measure of the importance of a specific input to output relationship. Therefore, these transformation invariant parameters are a central clue into which states should be included.

Various ideas for deciding how many modes take into account the operation of the system can be employed. One method is to observe carefully the output(s) of interest in a simulation. Then, the number of modes to keep can be iteratively decreased until unacceptable error is observed in the output of concern. Further the idea of the “scree” test can be used to determine how many principal components of the system are “true” principal components. The controller plays a role in the overall closed-loop system and must be included in the decision of how many modes to maintain.

Model Reduction Technique's Relative Effectiveness

The idea of a model reduction technique's effectiveness is meaningless unless the constraints for the system are well understood. In the first chapter the rational for reducing the number of POD basis vectors used in the temporal model included checking that the flow (solution) resulting from the full order finite-difference model was similar to the flow (solution) resulting from the reduced temporal model.

The comparison of the standard balanced truncation and the Hankel optimal norm approximation of the POD model show a definite difference between the two methods ability to match the full order system's output. Primarily the output of the first mode is the most important in the truncation process, which based upon the relative magnitudes of the outputs, clearly is the most important output mode.

The empirical balanced truncation gave very good results when compared with the linearized temporal system model. A benefit of using this method is that the input to output behavior is used to determine the approximated realization. The POD method of model creation usually needs a large set of solution snapshots that gather the input to state information. The POD method used a finite difference model to find solutions to the problem statement. The empirical method has the benefit that a system can be reproduced simply by observing the input-output behavior and does not require detailed knowledge of the system model *a priori*.

One further consideration that was not explored extensively in this thesis is the determination of frequencies that are most important for the control of the physical system. An understanding of the frequencies that are most importance to the physical system under consideration can allow for a weighting method to prioritize states for the model reduction process. Then, the model reduction problem can be reposed in the following way.

$$\min \left\| W_{out}(G - G_r)W_{in} \right\| \tag{8.1}$$

in some norm, where W_{out} and W_{in} are the output and input weighting functions respectively. Then, these weighting functions can be used for placing performance requirements based upon frequency into the model reduction problem. Additionally, using an infinite bandwidth controller can excite instabilities as found in [44]. Therefore, the frequencies of operation for the closed loop system are very important.

Future Research Opportunities

Several important opportunities exist for future research in the area of aerodynamic flow applications. Hopefully methods of control and system identification can possibly be modified to function for the Navier-Stokes equations as computing power increases in the future. Further, these advances could be applied to model reduction or controller reduction techniques in general. One promising area based upon past trends is an increase in computer computation power and available memory. Effectively using increased computational power so that additional states can be preserved for the control design process would allow for very detailed understanding of the closed loop system. The ‘design then reduce’ method might then be practical to use in many more applications. In fact, it would be very beneficial to look at an entire full order system model and controller interactions. Simulations could be performed and a very good method for controller reduction might be found. Then, all of the closed-loop system dynamics could be understood very well in simulation. In this way, model reduction would be unnecessary and only controller reduction with the full order system model would be analyzed.

Pure mathematics research into finding explicit closed form solutions to the Navier-Stokes equations is certainly an area that would benefit the aerodynamics community by allowing researchers to model more complex geometric shapes.

Perhaps an easier challenge will be to devise more efficient numerical analysis methods for better evaluating PDEs. The inherent ability of computers to operate efficiently on discrete portions of the domain space, might allow for analysis of the problems in an optimal order and partitioning of the problems solution.

Further, there is an extension to apply the empirical balanced truncation method to the full nonlinear two-dimensional or higher order Navier-Stokes equations. Some work has been done to develop a method to find nonlinear empirical Gramians that can be used to directly apply a balanced truncation method on the nonlinear model [37].

Additionally, the favorable results seen from empirical balanced truncation might be expanded such that a type of empirical Hankel optimal norm approximation could be formed. The standard methods of Hankel optimal norm approximation cannot be applied directly to a nonlinear temporal model such as (1.25). A generalized Hankel operator that can be applied to the PDE would allow for a theoretically better system realization than the balanced truncation method for a fixed number of states.

LIST OF REFERENCES

[1] Atwell, J. A., Borggaard, J. T., King, B. B., “Reduced Order Controllers For Burgers' Equation With A Nonlinear Observer”, Int. J. Appl. Math. Computational Science., 2001, Vol.11, No.6, pgs. 1311-1330.

[2] Bachelder, E. N. and Klyde, D. H., “Wavelet-based Analysis of Roll Ratchet Using A Flight Test Database”, Atmospheric Flight Mechanics Conference Austin, Texas 11-14 August 2003.

[3] Caicedo, J. M., Dyke, S. J., and Jonson, E. A., “Natural Excitation Technique and Eigensystem Realization Algorithm for Phase 1 of the IASC-ASCE Benchmark Problem: Simulated Data”, Journal of Engineering Mechanics, January 2004, pgs. 49-60.

[4] Camphouse, Chris R. and James H. Myatt, “Reduced Order Modelling and Boundary Feedback Control of Nonlinear Convection”, in American Institute of Aeronautics and Astronautics Guidance, Navigation, and Control Conference. 2005.

[5] Camphouse, R. C., Djouadi, S. M., and Myatt, J. H., “Feedback Control for Aerodynamics”. IEEE Conference on Decision and Control, Dec 2006.

[6] Dullerud, G. E. and Paganini, F., *A Course in Robust Control Theory: A Convex Approach*, Springer Science+ Business Media, 2000.

[7] Efe, M. O. And Ozbay H., “Proper Orthogonal Decomposition for Reduced Order Modeling: 2D Heat Flow”, IEEE, 2003.

[8] Elkin, V. I., *Reduction of Nonlinear Control Systems: A Differential Geometric Approach*, Kluwer Academic Publishers, 1997.

[9] Glover, K., "All Optimal Hankel-norm Approximations of Linear Multivariable Systems and Their L_∞ – Error Bounds," *International Journal of Control*, vol. 39, pp. 1115-1193, 1984.

[10] Holmes, P., Lumley, J. L., Berkooz, G., *Turbulence, Coherent Structures, Dynamical Systems and Symmetry*, Cambridge University Press, 1996.

[11] Hui-chuan, S., “Exact Solutions of Naiver-Stokes Equations – The Theory of Functions of a Complex Variable Ander Dirac-Pauli Representation and its Application in Fluid Dynamics (II)”, Applied Mathematics and Mechanics, Vol 7. No. 6, June 1986.

[12] Ilak, M. and Rowley, C. W., “Reduced-Order Modeling of Channel Flow Using Traveling POD and Balanced POD”, AIAA Flow Control Conference, 5-8 June 2006.

[13] Chung, T. J., *Computational Fluid Dynamics*, Cambridge University Press, 2002.

[14] Lall, S., Marsden, J. E., Glavaski, S. , “A Subspace Approach to Balanced Truncation for Model Reduction of Nonlinear Control Systems”, International Journal of Robust and Nonlinear Control, 2002; No. 12, pages 519-535.

[15] Lawrence, D. A., Myatt, J. H., and Camphouse, R. C., “On Model Reduction via Empirical Balanced Truncation”, American Control Conference, June, 2005.

[16] Leibfritx, F. and Volkwein, S. , “Numerical feedback controller design for PDE systems using model reduction: techniques and case studies”. Real-Time PDE-Constrained Optimization, SIAM, 2006.

[17] Balas, G. J., and Doyle, J. C., “Robustness and Performance Tradeoffs in Control Design for Flexible Structures.” Proceedings of the 29th Conference on Decision and Control, Honolulu, Hawaii Dec., 1990.

[18] Mathworks, “Partial Differential Equations Toolbox Help”. [Available Online: http://www.mathworks.com/access/helpdesk/help/toolbox/pde/]

[19] Rowley, C. W., Colonius, T., Murray, R. M., “Model reduction for compressible flows using POD and Galerkin projection.” Physica D, 189 (2004), pages 115-129.

[20] Rugh, W. J., *Linear System Theory*, Prentice Hall, Second Edition, 1996.

[21] Sohr, H., *The Naiver-Stokes Equations: An Elementary Functional Analytic Approach*, Birkhauser Verlag, 2001.

[22] Zhou, K., Doyle, J.C., and Glover, K., *Robust and Optimal Control*, Prentice Hall, 1996.

[23] Zhou, K. and Doyle, J. C., *Essentials of Robust Control*, Prentice Hall, 1998.

[24] Camphouse, R. C., “Boundary Feedback Control Using Proper Orthogonal Decomposition Models”, Journal of Guidance, Control, and Dynamics, vol 28, no 5, September-October, 2005.

[25] Juang, J., *Applied System Identification*, Prentice Hall, 1994.

[26] Tennekes, H. and Lumley, J. L., *A First Course in Turbulence*, The Massachusetts Institute of Technology, 1972.

[27] Lawrence, D. A., “Empirical Model Reduction for Active Closed-Loop Flow Control”, Final Report for Faculty Summer Research Opportunity, ARL Ohio, 2004.

[28] Banks, H., del Rosario, R., and Smith, R., Reduced Order Model Feedback Control Design: Numerical Implantation in a Thin Shell Model, Technical Report CRSC-TR98-27, Center for Research in Scientific Computation, North Carolina State University, June, 1998.

[29] Caraballo, E., Samimy, M., and DeBonis, J., Low Dimensional Modeling of Flow for Closed-Loop Flow Control,'' AIAA Paper 2003-0059, January 2003.

[30] Carlson, H., Glauser, M., Higuchi, H., and Young, M., POD Based Experimental Flow Control on a NACA-4412 Airfoil, AIAA Paper 2004-0575, January 2004.

[31] Carlson, H., Glauser, M., and Roveda, R., Models for Controlling Airfoil Lift and Drag, AIAA Paper 2004-0579, January 2004.

[32] Cohen, K., Siegel, S., McLaughlin, T., and Myatt, J., Proper Orthogonal Decomposition Modeling of a Controlled Ginzburg-Landau Cylinder Wake Model, AIAA Paper 2003-2405, January 2003.

[33] Willcox, K. and Peraire, J., Balanced Model Reduction via the Proper Orthogonal Decomposition, AIAA, Vol. 40, No. 11, November 2002, pp. 2323-2330.

[34] Sumali, Hartono, A New Adaptive Array of Vibration Sensors, Virginia Polytechnic Institute and State University, Ph. D. Dissertation, 1997.

[35] Graham, W. R., Peraire, J., Tang, K. Y., “Optimal Control of Vortex Shedding Using Low-Order Models. Part I—Open-Loop Model Development,” International Journal for Numerical Methods in Engineering, 44, pp. 945-972, 1999.

[36] Hahn, J. and Edgar, T. F., “Reduction of nonlinear models using balancing of empirical Gramians and Galerkin projections,” Proceedings of the American Control Conference, June 2000.

[37] Condon, M. and Ivanov, R., “Empirical Balanced Truncation of Nonlinear Systems,” Journal of Nonlinear Science. Vol. 14: pp. 405-414, 2004.

[38] Sirovich, L., “Turbulence and the Dynamics of Coherent Structures, Parts I-III,” Quarterly of Applied Mathematics, Volume 45, Brown University, Rhode Island, pp. 561-590, 1987.

[39] Moore, B. C., “Principal Component Analysis in Linear Systems: Controllability, Observability, and Model Reduction,” Transactions on Automatic Control, pp. 17-32, 1981.

[40] Karhunen, K., “Zur Spektraltheorie Stochastischer Prozesse”, Annales Academiæ Scientiarum Fennicæ, 1946.

[41] Loéve, M. M., *Probability Theory*, Princeton, NJ: VanNostrand, 1955.

[42] Hotelling, H., “Analysis of a Complex of Statistical Variables Into Principal Components”, Journal of Educational Psychology, pp. 417-441, 1933.

[43] Cattell, R. B., “The Scree Test for the Number of Factors”, Multivariate Behavioral Research, 1:245-76, 1966.

[44] Greene, C. S., and Willsky, A. S., “An Analysis of the Multiple Model Adaptive Control Algorithm,” 19th IEEE Conference on Decision and Control including the Symposium on Adaptive Processes, 1980.

[45] Kung, S. Y., “Optimal Hankel-norm Model Reductions: Scalar Systems,” in Proceedings 1980 Joint Automatic Controls Conference., San Francisco, CA, Paper FA8.A, August 1980.

[46] Kung, S. Y. and Lin, D. W., “Optimal Hankel-norm Model Reductions: Multivariable Systems,” IEEE Transactions on Automatic Control, vol. 26, pp. 832-852, 1981.

[47] Anderson, B. D. O., “Controller Design: Moving from Theory to Practice,” IEEE Control Systems Magazine, pp. 16-25, 1993.

[48] Atwell, J. A., “Proper Orthogonal Decomposition for Reduced Order Control of Partial Differential Equations,” Ph.D. Dissertation, Virginia Polytechnic Institute and State University, 2000.

[49] Camphouse, R. C. and Myatt J. H., “Feedback Control for Two-Dimensional Burger’s Equation System Model,” Proceedings on the 2nd Flow Control Conference on Control Applications, Portland, OR, 2004.

[50] Gu, G., “All Optimal Hankel-Norm Approximations and Their L_∞ Error Bounds in Discrete-Time,” Proceedings of the 41st IEEE Conference on Decision and Control, Las Vegas, Nevada, Dec. 2002.

[51] Lennart, L., *System Identification – Theory For the User*, 2nd ed, PTR Prentice Hall, Upper Saddle River, N.J., 1999.

[52] Elgar, P., *Sensors for Measurement and Control*, Prentice Hall, Upper Saddle River, N.J., 1998.

[53] Pintelon, R. and Schoukens, J., *System Identification: A Frequency Domain Approach*, Wiley-IEEE Press, 2001.

VITA

Jason Foster was born in Huntsville, Alabama. He moved to Lincoln County, Tennessee when he was 8 years old. After graduating from Lincoln County High School, he went to Tennessee Technological University (TTU) where he studied Electrical Engineering. Jason was very involved with TTU's IEEE student branch holding both the offices of publicity director (2002-2003) and vice-chair (2003-2004). Then after graduating with a Bachelor of Science degree in Electrical Engineering he worked for a semester at Oak Ridge National Laboratory (ORNL) as an Undergraduate Science Laboratory Internship (SULI) student. Then, he started his graduate studies at the University of Tennessee, Knoxville. He continued his tenure at ORNL under the Higher Education Research Experience (HERE) program and he continued his studies in control systems. He graduated from the University of Tennessee with a Master of Science degree in Electrical Engineering in 2007.